1 # Formation of flavone-based wooly fibres by glandular

2 # trichomes of *Dionysia tapetodes*.

3

4 Matthieu Bourdon[1†], Josephine Gaynord[2†], Karin Müller[3], Gareth Evans[1]

5 Simon Wallis[4], Paul Aston[4], David R. Spring[2], Raymond Wightman[1*]

6

7

8 [1]The Sainsbury Laboratory, University of Cambridge, Bateman Street, Cambridge,

9 CB2 1LR. UK

10 [2] Department of Chemistry, University of Cambridge, Lensfield Road, Cambridge,

11 CB2 1EW. UK.

12 [3] Cambridge Advanced Imaging Centre, Department of Physiology, Development

13 and Neuroscience, Downing Street, Cambridge, CB2 3DY, UK

14 [4] Cambridge University Botanic Garden, 1 Brookside, Cambridge, CB2 1JE. UK

15

16 [†]These authors contributed equally

17 *correspondence raymond.wightman@slcu.cam.ac.uk

18

19

Abstract

21

Dionysia tapetodes, a small cushion-forming mountainous evergreen in the Primulaceae, possesses a vast surface-covering of long silky fibres forming the characteristic "wooly" farina. This contrasts with some related *Primula* which instead possess a powdery farina. Using a combination of cell biology and analytical chemical techniques, we provide a detailed insight of wooly farina formation by glandular trichomes that produce a mixture of flavone and substituted flavone derivatives, including hydroxyflavones. Conversely, our analysis show that the powdery form consist almost entirely of flavone . The wooly farina in *D. tapetodes* is extruded through specific sites at the surface of the glandular head cell, characterised by a small complete gap in the plasma membrane, cell wall and cuticle. The data is consistent with formation and thread elongation occurring from within the cell. The putative mechanism of wool thread formation and its stability is discussed.

33

34

Keywords

36
Cell wall*, Dionysia*, farina, flavone, glandular trichome, hydroxyflavone, *Primula*, vacuole, wool

39
40

41 **Introduction**

42

43 The genus *Dionysia* contains 55 species, found across central Asia. They are very closely

44 related to *Primula* and some species have historically moved backwards and forwards

45 between the two genera (Lidén 2007). Under the Angiosperm Phylogeny Project, *Dionysia*

46 has been subsumed into *Primula* (https://www.mobot.org). However, the current

47 Missouri/Kew "Plant list", a working list of all plant species, still recognises *Dionysia* as a

48 genus in its own right (http://www.theplantlist.org). Species of *Dionysia* are dwarf shrubs or

49 woody perennials forming loose to densely compact cushions with terminal inflorescences.

50 They grow at high altitude in mountain regions usually on limestone cliffs although granite,

51 sandstone and dolomitic sites have also been recorded and are found in shaded or semi

52 shaded conditions. *Dionysia tapetodes* (Bunge 1871) is the most widely distributed *Dionysia*

53 with a range from the Kopet Dagh through NE Iran (mountains of Khorasan Province) to the

54 mountains of Afghanistan (Grey-Wilson 1989). This wide range helps to explain the variation

55 within the species. They form large, rather flat cushions with yellow flowers in the wild and in

56 cultivation (Beckett *et al.* 1993).

57 For some species of *Primula* and *Dionysia*, a mealy deposit termed farina (latin "meal" or

58 "flour") is found to cover all or a subset of aerial parts of the plant. It is readily observed, for

59 example on the leaf surface, either as a powder or, in some *Dionysia* species, as fine thread

60 (or wool)-like fibres that are commonly referred to as "wooly farina". Like *Primula*, in *Dionysia*

61 both farinose and efarinose forms can exist within the same species. The powdery farina of

62 *Primula* species is mostly comprised of 2-phenyl-4H-chromen-4-one, more commonly known

63 as flavone (Müller 1915; Blasdale 1945). Chemical analysis of solvent-rinsed plant organs

64 reveal a growing number of additional substituted flavones, particularly hydroxy- and

65 methoxy- derivatives. The number of different flavone types can be extensive and their

66 presence/absence can vary between closely-related species (Valant-Vetschera *et al.* 2009,

67 2010; Bhutia *et al.* 2013; Hinterdobler *et al.* 2017). Given these flavone assignments

68 represent total surface-extracted flavones that include different tissue/cell types, it is not

69 clear which substituted flavones actually constitute the farina of a given species.

70 Farina biosynthesis takes place in glandular trichomes that typically consist of a stalk

71 attached to a single round cell known as the glandular head (Fico *et al.* 2007; Vitalini *et al.*

72 2011; Bhutia and Valant-Vetschera 2012). The crystals of powdery farina are seen to coat

73 the head cell and, at the subcellular level, a proliferation of smooth ER is observed

74 suggesting a site of synthesis and transport of some biosynthetic intermediates

75 (Wollenweber and Schnepf 1970; Gunning and Steer 1996). Part of the biosynthetic

76 pathway to flavones is known but for synthesis of more complex derivatives is less well

77 understood (Jiang *et al.* 2016). Chalcone synthase (CHS) represents the first step in the

78   flavonoid biosynthetic pathway and immunolocalization of the enzyme in farinose *Primula*

79   *kewensis* shows high signal in the gland head cell (but not in an *efarinose* mutant),

80   suggesting the full flavone farina biosynthetic machinery is present in this cell (Schopker *et*

81   *al.* 1995). Furthermore, immunogold labelling showed enrichment of CHS in spherical bodies

82   in the cytoplasm. As flavone farina biosynthesis continues, the subcellular locations of

83   intermediates and final products are not known. Generally, flavone glycones, being soluble,

84   can accumulate in the vacuole (Marinova *et al.* 2007) but, for farina producing plants, the

85   storage location of the insoluble aglycone is not well understood, possibly being localised to

86   a modified vacuole-type organelle that can stretch across the cell (van Brederode and

87   Steyns 1985). These flavone and flavone-type aglycones need to be transported out of the

88   cell and through the cell wall and cuticle for deposition on the surface of the hair cell.

89   Presumably this becomes more complicated for wooly farina whereby the flavone building

90   blocks need to be concentrated to a single exit site to produce an elongating fibre.

91   We present here our results showing wooly farina composition and the subcellular

92   organisation of the glandular trichome head cell that is the site of farina synthesis in *D.*

93   *tapetodes*. We identify the wool as a mixture that includes flavone and hydroxyflavones that

94   emerge from the head cell and is threaded through distinct gaps in the cell wall and cuticle.

95   The mechanism of wool formation is discussed.

96

97   **Materials and Methods**

98

99   Plant propagation and harvesting.

100

101   We used *Dionysia tapetodes* accession 20140435 that was received from the Royal Botanic

102   Garden Edinburgh (accession 19822508) comprising wild material collected by Prof. T.F.

103   Hewer (number 1164) between 1969 and 1971. *D. tapetodes* was grown at Cambridge

104   University Botanic Garden (Cambridge, UK) in clay pots plunged in sand in an alpine house

105   to keep the roots cooler and at a more stable temperature. The potting compost comprised

106   50% loam-based compost, 30% 1-9mm grit, 10% sharp sand, 10% seramis and a small

107   amount of slow release fertiliser. The compost is top-dressed with grit which is carefully

108   worked under the collar of the plant to reduce the risks of basal rot. Given that *Dionysia* are

109   prone to rosette burning from overexposure to sunlight, a temporary shading screen was

110   placed over the collection from mid-March and removed later in the season after sun

111   intensity decreased. Old flowers were carefully removed to prevent any botrytis infection

112   moving from dead flowers into living material. Watering adhered to a strict regime: Young

113   plants were watered from underneath via a water bath and once they passed one year old

114 were then watered overhead without getting the cushion surface wet. Water was applied

115 sparingly in the winter months and increased once the plants were in active growth.

116

117 <u>Cryo-Scanning Electron Microscopy (cryoSEM) and cryo-fracture.</u>

118

119 Rosettes of 5-8 leaves were mounted, frozen in nitrogen slush, platinum coated and

120 fractured as previously described (Wightman *et al.* 2018). To accommodate better fractures

121 without dislodging trichomes, some samples were dipped in 70% v/v ethanol to remove the

122 wool and then air-dried prior to freezing. Cryo prepared samples were viewed using a Zeiss

123 EVO HD SEM fitted with a backscattered electron detector and 25 kV acceleration voltage.

124

125 <u>Low kV SEM imaging of wool fibres.</u>

126

127 Clumps of uncoated wool fibres were placed on a sticky carbon tab and mounted on an SEM

128 stub in the Zeiss EVO HD SEM at high vacuum and 1kV accelerating voltage using SE

129 detector fast scanning with frame averaging to prevent wool movement.

130

131 <u>Embedding, sectioning and imaging of trichomes by transmission electron microscopy</u>

132 <u>(TEM) and light (epifluorescence) microscopy.</u>

133

134 Leaves were dissected with razor blades in a solution consisting of 4% formaldehyde

135 (freshly prepared from paraformaldehyde powder, Sigma) and 0.5% glutaraldehyde (Sigma)

136 in PBS buffer. Fixation, dehydration, resin infiltration and antibodies washing steps were all

137 microwave (MW) assisted using a PELCO BioWave Pro (Ted Pella). Fixation was realized at

138 150W, under vacuum (20Hg) (5x 1min). Samples were left in the fixative overnight at 4°C

139 and then washed 3 times in PBS. Stems were then parallelly aligned and embedded in 1%

140 agarose in PBS. Samples were then processed through increasing dehydration steps (25%,

141 50%, 70%, 90%, 96%, 3x 100% ethanol, vacuum 20Hg, MW 150W 5min), and left overnight

142 in 100% ethanol at 4°C. Resin infiltration (LR White medium grade, Agar scientific) was then

143 realized through increasing resin concentration: 33% Resin in ethanol 100%, 66% Resin in

144 ethanol 100%, and 3 times 100% Resin (20Hg, MW 200W 5min). Samples were left at least

145 24h in 100% resin for effective penetration in the samples. Resin polymerization was

146 subsequently realized at 60°C during 18h.

147 For epifluorescence microscopy, semi-thin sections (1μm) of the whole leaf bud were then

148 obtained with a Leica EM UC7 ultramicrotome using a Histo Jumbo 8mm diamond knife

149 (DiATOME) and laid on droplets of sterile water on uncoated glass microscopy slides. In

150 order to avoid folds on sections during the water drying process, slides were dried on a hot

151   plate at 55°C (Leica). Slides were finally mounted in a 1:1 solution of AF1 antifadent

152   (Citifluor) with PBS, containing calcofluor as a cell wall counterstaining, and imaged by

153   confocal laser scanning microscopy (Zeiss LSM700).

154   For TEM observations, 100nm thin sections were obtained with a Leica EM UC7

155   ultramicrotome using an ultra 45° diamond knife (DiATOME) and deposited on 200-300µm

156   mesh formvar-coated nickel grids

157   Samples were post-stained using Reynold's lead citrate and uranyl acetate for 3 min in

158   each. Thin sections were viewed in a FEI/Thermofisher Tecnai G20 electron microscope run

159   at 200 keV with a 20 µm objective aperture to improve contrast. Images were taken with an

160   AMT camera running DEBEN software.

161

162   <u>Field Emission Scanning Electron Microscopy (FE-SEM) of leaf sections.</u>

163

164   Whole rosettes were dissected with razor blades to remove apical parts of leaves and

165   immediately submerged in fixative (2 % glutaraldehyde/2 % formaldehyde in 0.05 M sodium

166   cacodylate buffer pH 7.4 containing 2 mM calcium chloride) under vacuum overnight at room

167   temperature. After washing 5x in DIW (deionised water), samples were osmicated (1 %

168   osmium tetroxide, 1.5 % potassium ferricyanide in 0.05 M sodium cacodylate buffer pH 7.4)

169   for 3 days at 4°C. Then samples were washed 5x with DIW and treated with 0.1 % (w/v)

170   thiocarbohydrazide/DIW for 20 minutes at room temperature in the dark. After washing 5x in

171   DIW, samples were osmicated a second time for 1 hour at RT (2% osmium tetroxide/DIW).

172   After washing 5x in DIW, samples were blockstained with uranyl acetate (2 % uranyl acetate

173   in 0.05 M maleate buffer pH 5.5) for 3 days at 4°C. Samples were washed 5x in DIW and

174   then dehydrated in a graded series of ethanol (50%/70%/95%/100%/100% dry) 100% dry

175   acetone and 100% dry acetonitrile, 3x in each for at least 5 min. Samples were infiltrated

176   with a 50/50 mixture of 100% dry acetonitrile/Quetol resin (without BDMA) overnight,

177   followed by 3 days in 100% Quetol (without BDMA). Then, the sample was infiltrated for 5

178   days in 100% Quetol resin with BDMA, exchanging the resin each day. The Quetol resin

179   mixture is: 12 g Quetol 651, 15.7 g NSA, 5.7 g MNA and 0.5 g BDMA (all from TAAB).

180   Samples were placed in embedding moulds and cured at 60°C for 3 days. Semi-thin

181   sections (1µm) of the whole leaf bud were then obtained with a Leica EM UC7

182   ultramicrotome using a Histo-Jumbo 8mm diamond knife (DiATOME) and laid on droplets of

183   sterile water on uncoated glass microscopy slides. In order to avoid folds on sections during

184   the water drying process, slides were dried on a hot plate at 55°C (Leica). Glass slides were

185   then resized with a glass knifemaker to be mounted on aluminium SEM stubs using

186   conductive carbon tabs, and the edges of the slides were painted with conductive silver

187   paint. Samples were sputter coated with 30 nm carbon using a Quorum Q150 TE carbon

188   coater. Samples were imaged in a Verios 460 scanning electron microscope

189   (FEI/Thermofisher) at 4 keV accelerating voltage and 0.2 nA probe current in backscatter

190   mode using the concentric backscatter detector (CBS) in immersion mode at a working

191   distance of 3.5-4 mm; 1536 x 1024 pixel resolution, 3 us dwell time, 4 line integrations.

192   Stitched maps were acquired using FEI MAPS software using the default stitching profile

193   and 10% image overlap.

194

195   <u>Measurements of wool fibre diameter.</u>

196

197   Images of wool fibres, attached to leaves of an isolated *D. tapetodes* rosette, were taken

198   with a Keyence VHX-7000 microscope at 2500x magnification and illuminated with full field

199   coaxial light. 2D depth-up mode was used for in-focus acquisitions. Fibre width

200   measurements were carried out using the point-to-point measuring tool in the Keyence

201   software.

202

203   <u>Raman microscopy of farina.</u>

204

205   Raman microscopy was carried out on a Renishaw InVia instrument equipped with a 785 nm

206   laser. *D. tapetodes* farina wool or *P. marginata* powder was carefully placed on a quartz

207   slide and brought in to focus under a 50x dry objective lens. Raman acquisitions used a

208   1200 l/mm grating, 1200 cm^{-1} centre, 785 nm laser at 10% power, regular confocal mode

209   and 4 s exposure with 3 accumulations. At least 3 spectra per sample were averaged in

210   order to improve signal-to-noise. To find close matches with reference Raman spectra, the

211   experimental spectra were used as a search input against the Raman databases, that

212   include some flavone derivatives, in the KnowItAll software (Bio-Rad Inc.) using the

213   "SearchIT" tool and then candidate spectra were visualised by eye to remove false positives.

214   Both default and Euclidean distance search settings were used. Matches are ranked

215   according to their hit quality index (out of a maximum of 100). *P. marginata* farina gave a

216   close match (97/100) with flavone. *D tapetodes* gave no close matches but yielded good

217   correlation (70-80/100) to reference spectra of hydroxy- and methoxy- flavone derivatives

218   that included 7, 2'-dimethoxyflavone; 3,7-dimethoxyflavone and 6-, 7-, or 8- hydroxy-

219   derivatives. For fastFLIM-Raman correlative imaging of leaves submerged in water

220   (Supplementary data Fig. S9) a confocal-Raman microscope, described in (Wightman *et al.*

221   2019), used the following settings: 25x 0.95 NA water dipping objective lens, FLIM 440 nm

222   pulsed laser (at 20 MHz) with detector window set between 448 nm and 511 nm and 80

223   iterations. Raman: 1200 l/mm grating, 1200 cm^{-1} centre, 785 nm laser, 50% power, 15 s

224   exposure with 2 accumulations used in line scan mode that intersected a glandular head

225   cell.

226

227   <u>Reagents, solvents and sample preparation for chemical analysis.</u>

228

229   Pure Flavone was purchased from Alfa Aesar as a white solid with 99% purity (CAS no. 525-

230   82-6, catalogue no. A13627) and used without further purification. All solvents were anhydrous

231   and used as purchased without any further purification. Flavone wool from was picked from

232   *D. tapetodes* leaf surfaces using fine tweezers and placed in a microcentrifuge tube. The wool

233   sample (approximately 0.5 mg) was dissolved in 50 µL of acetonitrile/water (1:1) with a few

234   drops of dimethylsulfoxide (DMSO) to aid solubility. Sample preparation was performed in this

235   way for analytical HPLC, LCMS and HRMS analysis.

236

237   <u>Analytical high-performance liquid chromatography (HPLC)</u>

238

239   Analytical HPLC was run on an Agilent 1260 Infinity using a Supelcosil ABZ+PLUS column

240   (150 mm × 4.6 mm, 3 µm) eluting with a linear gradient system (solvent A: 0.05% (v/v)

241   trifluoroacetic acid (TFA) in H_2O, solvent B: 0.05% (v/v) TFA in acetonitrile (MeCN)) over 15

242   min at a flow rate of 1 mL/min.

243

244   <u>Liquid chromatography mass spectrometry (LCMS)</u>

245

246   Chromatographs were recorded on a Waters ACQUITY H-Class UPLC with an ESCi Multi-

247   Mode ionisation Waters SQ Detector 2 spectrometer (LC system: solvent A: 2 mM ammonium

248   acetate in water/MeCN (95:5); solvent B: 100% MeCN; column: AQUITY UPLC CSH C18,

249   2.1*50 mm, 1.7 µm, 130 Å; gradient: 63 5-95% B over 3 min with constant 0.1% formic acid).

250

251   <u>High resolution mass spectrometry (HRMS)</u>

252

253   HRMS was carried out on a Waters LCT Premier Time of Flight mass spectrometer. ESI refers

254   to the electrospray ionisation technique.

255

256   <u>Nuclear magnetic resonance (NMR) spectroscopy</u>

257

258   All pulse sequences are the default (with the exception of the DEPT135) from the Topspin

259   3.2pl7 software used to control the acquisition. The analysis required ^{1}H, ^{13}C, DEPT135, DFQ-

260   COSY, Heteronuclear Single Quantum Coherence (HSQC, with DEPT 135 editing) and

261 Heteronuclear Multiple Bond Correlation Spectroscopy (HMBC) spectra. All necessary
262 shaped and decoupling pulses were calculated by the software, using defined 90 degree
263 pulses.

264 ^{1}H NMR: Proton magnetic resonance spectra were recorded using an internal deuterium lock
265 (at 298 K unless stated otherwise) on Bruker DPX (400 MHz; ^{1}H-^{13}C DUL probe), Bruker
266 Avance III HD (400 MHz; Smart probe), Bruker Avance III HD (500 MHz; Smart probe) and
267 Bruker Avance III HD 62 (500 MHz; DCH Cryoprobe) spectrometers. Pulse sequence used
268 zg30 – PLW1=14W, P1=10.5µs, SW=20 ppm, TD=64 K, AQ=3.28 s, D1=1 s, NS=16. Proton
269 assignments are supported by ^{1}H-^{1}H COSY, ^{1}H-^{13}C HSQC or ^{1}H-^{13}C HMBC spectra, or by
270 analogy. Chemical shifts (δH) are quoted in ppm to the nearest 0.01 ppm and are referenced
271 to the residual non-deuterated solvent peak. Discernible coupling constants for mutually
272 coupled protons are reported as measured values in Hertz, rounded to the nearest 0.1 Hz.
273 Data are reported as: chemical shift, multiplicity (br, broad; s, singlet; d, doublet; t, triplet; q,
274 quartet; m, multiplet; or a combination thereof), number of nuclei, coupling constants and
275 assignment.

276 ^{13}C NMR: Carbon magnetic resonance spectra were recorded using an internal deuterium
277 lock (at 298 K unless stated otherwise) on Bruker DPX (101 MHz), Bruker Avance III HD (101
278 MHz) and Bruker Avance III HD (126 MHz) spectrometers with broadband proton decoupling.
279 1024 scans (NS) were acquired using pulse sequence 'zgpg30', with waltz16 1H decoupling.
280 90 degree 13C pulse set to 21W (PLW1) for 9.5 µs (P1). 209786 points (TD) were digitised
281 over 3.02 s (AQ), relaxation delay set to 2 s (D1). Sweep width was 276 ppm (SW), with an
282 irradiation frequency of 110 PPM (O1P). Carbon spectra assignments are supported by DEPT
283 editing, ^{1}H-^{13}C HSQC or ^{1}H-^{13}C HMBC spectra, or by analogy. Chemical shifts (δC) are quoted
284 in ppm to the nearest 0.1 ppm and are referenced to the deuterated solvent peak. Data are
285 reported as: chemical shift, number of nuclei, multiplicity, coupling constants and assignment.
286 Magnetic resonance spectra were processed using TopSpin (Bruker). An aryl, quaternary, or
287 two or more possible assignments were given when signals could not be distinguished by any
288 means. Standard flavone numbering was followed.

289 DEPT 135: Pulse sequence dept135sp – This is a minor modification of the DEPT sequence
290 to optimise the spectral baseline and uses an adiabatic shape for 180 degree carbon pulses.
291 Carbon pulse powers as ^{13}C experiment above, SW=236.7 ppm, TD=65536, AQ=1.10 s,
292 D1=2 s, O1=100 ppm, NS=64. Waltz16 decoupling.

293 DFQCOSY: This is a double-quantum filtered experiment; using gradient selection; pulse
294 sequence cosygpmfqf. Non-uniform sampling; using a Poisson-gap weighted schedule was
295 used to acquire 37.5% of 512 increments, each with 2 scans (SWF2=13.37 ppm, TD=4k,
296 AQ=0.31 s, D1=2 s). Proton pulse powers as above. Processed to 2k x2k points using a sine
297 function (SSB=2.5)

298   HMBC: This experiment is phase sensitive; uses Echo/Antiecho gradient selection, with a

299   three-fold low-pass J-filter to suppress one-bond correlations; pulse program 'hmbcetgpl3nd'.

300   Acquired in phase sensitive mode using Echo/Antiecho-TPPI gradient selection, with a 3 step

301   low pass j-filter to suppress 1 bond correlations. Long-range J-JCH parameters set to 10 Hz.

302   Non-uniform sampling; with a Poisson--gap weighted schedule was used to acquire 37.5% of

303   768 increments; each with 2 scans (SWF1=250, SWF2=12.02 ppm, TD=4096, AQ=0.34 s,

304   D1=2 s). Processed to 2048x2048 using a sine function (SSB=4 & 2 for F2 and F1), then

305   converted to magnitude mode in F2. (Topspin command 'xf2m')

306   HSQC: The HSQC was acquired using a Bruker Avance III HD 500Mhz equipped with a dual

307   13C/1H cryoprobe; using Topspin 3.2pl7. It was acquired in 'non-uniform sampling' mode and

308   samples 25% of 1024 increments, using a 'poisson-gap' schedule. The data was processed

309   using the default compressed sensing (CS) method in Topspin 3.5pl7 (on your computer) to

310   2048x2048 data points. This experiment is configured to give -CH2 groups an opposite phase

311   to the -CH and -CH3 groups, using the hsqcedetgpsp.3 pulse sequence. Acquired in phase

312   sensitive mode using Echo/Antiecho-TPPI gradient selection, multiplicity edited during

313   selection step with shaped adiabatic pulses. Non-uniform sampling; with a Poisson-gap

314   weighted schedule was used to acquire 25% of 1024 increments; each with 2 scans

315   (SWF1=190 ppm, SWF2=12.99 ppm, TD=1816, AQ=0.14 s, D1=0.8 s). Carbon and proton

316   pulse powers as above. Processed to 2048x2028 points using a qsine function (SSB=2).

317   Standard flavone numbering:
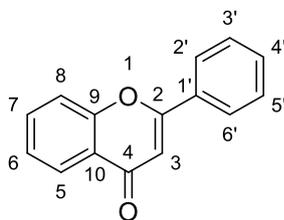
318
319
320

321

322

323

324   **Results**

325

326   <u>Wooly farina fibres of *Dionysia tapetodes* have distinct surface grooves and differ in</u>

327   <u>composition to powdery farina.</u>

328

329   *D. tapetodes* grows as a densely packed cushion (Fig. 1A) with large quantities of "wooly"

330   fibres observed on both the adaxial and abaxial surface of the *D. tapetodes* leaf (Fig. 1B).

331   Wooly farina production likely occurs throughout leaf growth since it is present in both young

332   leaves (found at the centre of the rosette) and older leaves (positioned on the outside of the

333   rosette). Farina production at early stages of growth are consistent with the observed

334   entanglement of fibres between neighbouring leaves as revealed by scanning electron

335   microscopy (SEM) (Fig. 1C). Individual wooly fibres range in width from 0.9 to 2.1 microns,

336   with a mean width of 1.6 microns (n=51). High magnification low kV SEM of uncoated fibres

337   shows fine grooves on their surface, making a series of ridges arranged longitudinally (Fig.

338   1D). In order to understand how these fibres are formed and maintained, we compared the

339   Raman spectra of wooly farina of *D. tapetodes* with the powdery farina found near the leaf

340   margin of *Primula marginata*. Figure 1E shows an overlay of the spectra from both farina

341   types. The powder spectrum of *P. marginata* matches that of pure flavone (see materials

342   and methods for details of spectra correlation), indicating that flavone makes up all or the

343   vast majority of the farina in this species. The spectrum of *D. tapetodes* wooly farina,

344   however, only shares some of the peaks with the flavone powder of *P. marginata*; at 674,

345   1001, 1012 and 1568 cm^{-1}. This suggests a substituted and/or mixture of flavones comprise

346   the wooly farina of *D. tapetodes*. Spectral search and correlation software were used to

347   identify candidate functional groups (see materials and methods) based on the acquired

348   Raman spectra and compared to a reference database that included some flavone

349   derivatives. While *P. marginata* farina correlated very highly with unsubstituted flavone (hit

350   quality index 97 out of a possible 100 maximum), *D. tapetodes* wooly farina gave no close

351   matches. However, the best hits (hit quality index 70-80) were to various combinations of

352   mono-and di- hydroxy- and methoxy- substituted flavones. This suggests that hydroxy-

353   and/or methoxy functional groups might co-exist with flavone in the wool fibres.

354

355   <u>The wooly farina of *D. tapetodes* comprises mostly flavone mixed with substituted flavones.</u>

356

357   A sample of the wooly farina from *D. tapetodes* was further analysed by high-performance

358   liquid chromatography (HPLC), liquid chromatography-mass spectrometry (LCMS), high-

359   performance mass spectrometry (HRMS) and nuclear magnetic resonance (NMR)

360   spectroscopy. All data are presented together with a detailed interpretation in Supplementary

361   dataset S1 that additionally comprises Supplementary data Figs. S1-S7 and Table S1. This

362   analysis revealed that the wooly farina sample was mainly composed of unsubstituted flavone

363   (>90% by analytical HPLC, structure A in Fig. 2). Identical analytical data was obtained for a

364   pure sample of flavone from a commercial source (Supplementary data dataset S1, Fig. S4).

365   The HPLC, LCMS and HRMS data indicated that there are other, substituted flavone species

366   present in the wooly farina sample; exactly how many other species is not clear. HPLC

367   analysis gave only one, whereas LCMS data suggested the presence of multiple other

368 flavonoids. Mass ions were observed in the LCMS corresponding to hydroxy- and methoxy-
369 substituted flavones (Supplementary data Figs. S1 and S2). To provide more information on
370 the structure of the minor flavone species, 2D NMR was carried out and yielded candidate
371 structures corresponding to 2'-hydroxyflavone and 4'-hydroxyflavone (Fig. 2, Supplementary
372 data Fig. S7).

373

374 The wool fibres emerge from distinct holes in the cell wall of the glandular trichome head cell
375 and are in close proximity to dense material of the vacuole.

376

377 Focal points representing the origin of numerous fibres can be seen on the *D. tapetodes* leaf
378 surface (Fig. 3A) corresponding to mature flattened glandular trichomes (Fig. 3B).
379 Interspersed between these locations are numerous smaller and extended trichomes that
380 have fewer, single or no wool fibres emerging from the head cells and likely represent
381 glandular trichomes at different levels of maturity (Fig. 3B and 3C). It is evident that, when
382 looking at the smaller trichomes, farina emerges from a few discrete locations on the
383 glandular head cell that may grow in number as the cell ages. This appears to be in contrast
384 to *P. marginata*, where smaller crystals completely cover the circumference of the head cell
385 (Fig. 3D). These data show that, for *D. tapetodes*, flavone incorporation and extrusion needs
386 to be sustained at the same site on the (head) cell surface. We used cryoSEM to observe,
387 close-up, the junction between wool fibre and cell (Fig. 4A, B) where the fibre appears to
388 come out of the cell wall. We generated random cryofractures through the leaf that might
389 include a glandular head cell, however, the interaction of the fracture knives with the wool
390 resulted in dislodging of the trichome from the leaf, as well as more cellular debris at the
391 fracture site. We found a 5 s wash with 70% v/v ethanol removed the surface wool and
392 resulted in better cryofractures with less debris. Sites of wool fibre extrusion, represented as
393 small "craters" on the cell surface, are visible after the washing (Fig. 4C). Cryofractures that
394 included any part of the gland head cell were, however, very rare. One fracture removed
395 most of the head cell leaving a part of the head and some cytoplasm intact (Fig. 4D).
396 Ethanol washing had removed the external wool fibres from the sample, however, a single
397 fibre is observed inside the cell that was protected from the solvent (red arrow in Fig. 4D).
398 This suggests the wool is made inside the cell and then somehow threaded through a gap in
399 the wall. A second fracture was obtained through the centre of the gland hair cell (Fig. 4E)
400 and a wool exit site could be observed close to the fracture plane. At this location the
401 vacuole appeared to be close to the surface with a small amount of cytoplasm in between
402 (Fig. 4F). Given that we could not obtain a fracture through the site of wool extrusion in the
403 cell wall, we carried out Transmission Electron Microscopy (TEM) on post-stained sections
404 of fixed glandular trichomes. TEM processing completely removes all the farina wool,

405   however, complete gaps in the cell wall were observed (Fig. 4G) and were in close proximity

406   to dense particulates that, based on the FE-SEM imaging described below, represent

407   contents of the vacuole. These gaps are not an artefact from masking or non-uniform

408   staining for TEM because they were also observed, in addition to the dense vacuoles, with

409   light microscopy (Supplementary data Fig. S8). A small amount of cytoplasm, as well as an

410   amorphous stained region, can be observed between the dense particulates and the cell

411   wall gap (Fig. 4H). A magnified TEM view of the wall shows a mesh structure with layers of

412   differing density that likely represent polysaccharide components including cellulose (Fig.

413   4I). A low density outer layer is present that is consistent with cuticular wax plus a thin

414   epicuticular layer on top (Fig. 4I). This was confirmed by correlative fluorescence lifetime

415   imaging and Raman microscopy which showed six Raman peaks (1062, 1132, 1294, 1416,

416   1438, 1465 cm^{-1}) that correspond to the major peaks of epicuticular waxes from Sorghum

417   (Farber *et al.* 2019). These wax peaks were specific to the outer surface of the gland hair

418   cell and were found together with the flavone-type signals (Supplementary data Fig. S9). An

419   intracellular store of flavone was also located.

420   In order to identify how the generation of a hole in the cell wall is coupled with directed

421   deposition of flavone to make a thread, we used a higher throughput approach for imaging

422   larger numbers of glandular trichomes. Full rosettes that include leaves at various stages of

423   development were stained, embedded and sectioned. These large area sections were

424   viewed by field emission scanning electron microscopy (FE-SEM) of backscattered electrons

425   and gave good contrast for observations of membranes. Out of 11 gaps examined, where

426   vacuoles could be easily distinguished from other organelles due to their intense staining, 6

427   gaps were within 1 µm of its closest vacuolar compartment with distances in the range 0 –

428   2.6 µm (mean 1.1 µm, median 0.72 µm). FE-SEM showed the gaps in the cell wall and

429   cuticle also includes the plasma membrane (Fig. 4J-L,); 15/15 gaps observed with FE-SEM

430   had no plasma membrane crossing the gap. For two glandular heads, we observed the gap

431   to extend further inside the cell as far as the vacuole and in one section the tonoplast was

432   intact (Fig. 4M, N). We observed fully formed trichomes where the dense staining was seen

433   in a void within the cell wall of width 1.15 µm consistent with the size expected of a forming

434   wool thread (Fig. 4O) and suggesting a careful coupling between wall digestion and

435   deposition of the flavone and derivatives.

436

437   **Discussion.**

438

439   *D. tapetodes* is covered with wooly farina around the leaves. It is not entirely understood

440   what the purpose of the farina is, however, tolerance to freezing and high UV have been

441   cited (Caldwell 1971; Sisa *et al.* 2010). Consistent with the latter, there exists an efarinose

442   *D. tapetodes* accession at the Cambridge University Botanic Garden and horticulturists

443   working closely with the plants report that it scorches more easily in the sun compared to the

444   farinose accessions.

445   The wooly farina threads radiate in all directions from mature glandular head cells of

446   trichomes that are interspersed on the leaf epidermis. In addition to biosynthesis, these head

447   cells appear to act as anchor points of the wool which can extend between adjacent leaves.

448   The study of wool farina formation in *D. tapetodes* is made challenging by the physical and

449   chemical characteristics of the wool itself. CryoSEM gave good preservation of wool and

450   cellular structure but despite numerous random cryo-fractures, an image of a thread exiting

451   the cell through the cell wall gap was never obtained. High resolution light and electron

452   microscopy of embedded and sectioned material gave the best images of the wool exit sites

453   and surrounding subcellular compartments, however, the processing removed the wool

454   threads (although dense vacuolar staining likely attributed to stores of flavones and

455   derivatives can be seen). Observing the gaps within the cuticle, cell wall, plasma membrane

456   and cytoplasm where the thread is presumed to exist, before processing, does give us clues

457   as to how the wool is made; we speculate that a small void in the wall, arising by digestion of

458   the wall constituents, begins on the side of the wall facing the cell (Fig. 5). Flavone material

459   from the vacuole is transported to and deposited into this void. Completion of digestion to

460   include the cuticle permits the flavone aggregate to then extrude outside the cell to form the

461   wool while forming a perfect seal with the edge of the hole (Fig. 5), helped by the large

462   amounts of epicuticular wax. For thread elongation, flavone is continually deposited to the

463   cytoplasmic (elongating) end and the thread can protrude deeper into the cell towards the

464   vacuole(s). This apparent vacuole fusion may arise due to rapid flavone transport and

465   deposition across the tonoplast.

466   A question remains as to how the wooly threads of farina are formed and stably maintained

467   where other flavone-based farina forms a powder. Our compositional analyses suggest the

468   *D. tapetodes* wool is predominantly flavone mixed with 2'- and 4'-hydroxyflavones plus small

469   quantities of other unidentified substituted flavones. The three identified flavones are not

470   unique to this species, since they are found among the powdery *Primula*, where they are

471   referred to as epicuticular flavonoids (Colombo *et al.* 2014). There are, however, data

472   supporting strong intermolecular H-bonding for the 2' and 4'-hydroxy positions compared to

473   weak H-bonds for the 6-hydroxy position and *intra*molecular bonds in 5-hydroxyflavone

474   (Looker and Hanneman 1962; Looker *et al.* 1966). These intermolecular interactions

475   between the 2' and 4'-hydroxyflavones and with the bulk flavone may be enough to maintain

476   the integrity of a wool thread. Our Raman data of the *P. marginata* powder show a match

477   with only flavone with no evidence of a mixture like that observed for *D. tapetodes* and so in

478   the former species promoting powder rather than wool extrusion seen in the latter. Despite

479 this observation, chemical analysis of exudate flavonoids demonstrate large quantities of

480 flavone and 2'-hydroxyflavone in *P. marginata* (Valant-Vetschera *et al.* 2009). We put

481 forward a hypothesis that, while a diversity of substituted flavones is maintained across

482 powdery and wooly farina forming species, only wooly farina species can correctly mix and

483 incorporate these at a single site of synthesis to make continuous threads. The selection

484 pressure(s) that have resulted in powdery vs wooly vs efarinose species is not understood,

485 however, the wool does appear to give better coverage over the whole plant while we

486 speculate that the fine loose powder, while more local and easier to dislodge, can yield a

487 denser coating. In addition to the reported capacity of flavonoids to provide protection

488 against UV and potentially during freezing events, the unique capacity of *D. tapetodes* for

489 threading flavones may provide another evolutionary step towards previously described

490 xeromorphic adaptation to drought in the genus *Dionysia* (Wendelbo 1971). Indeed, such

491 specific spatial deposition of flavones seems to offer more leaf coverage from a single

492 production point (glandular trichome), which may limit air movement on the leaf surface,

493 therefore limiting water loss. It remains to be seen whether the properties of wooly farina

494 might make it a useful industrial biomaterial.

495

496 **Acknowledgements.**

497

506

507 **References.**

508

509 **Beckett KA, Grey-Wilson C, Alpine Garden Society (Great Britain)**. **1993**. *Encyclopaedia*

510 *of alpines*. AGS Publications.

511 **Bhutia TD, Valant-Vetschera KM**. **2012**. Diversification of Exudate Flavonoid Profiles in

512 Further Primula spp. *Natural Product Communications* **7**: 587–589.

513 **Bhutia TD, Valant-Vetschera KM, Brecker L**. **2013**. Orphan Flavonoids and

514 Dihydrochalcones from Primula Exudates. *Natural Product Communications* **8**: 1081–1084.

515 **Blasdale WC**. **1945**. The Composition of the Solid Secretion Produced by Primula

516   Denticulata. *Journal of the American Chemical Society* **67**: 491–493.

517   **van Brederode J, Steyns J**. **1985**. UV-microscopic studies on the vacuolar changes caused

518   by the flavone "aglycone" isovitexin inSilene pratensis plants. *Protoplasma* **128**: 59–63.

519   **Bunge A**. **1871**. Die Arten der Gattung Dionysia Fenzl. *Bull. Acad. Imp. Sci. St. Petersburg*

520   **16**: 547–563.

521   **Caldwell MM**. **1971**. Solar UV irradiation and the growth and development of higher plants.

522   *Photophysiol Curr Top*.

523   **Colombo PS, Flamini G, Christodoulou MS, *et al.* 2014**. Farinose alpine Primula species:

524   Phytochemical and morphological investigations. *Phytochemistry* **98**: 151–159.

525   **Farber C, Li J, Hager E, *et al.* 2019**. Complementarity of Raman and Infrared Spectroscopy

526   for Structural Characterization of Plant Epicuticular Waxes. *ACS Omega* **4**: 3700–3707.

527   **Fico G, Rodondi G, Flamini G, Passarella D, Tomé F**. **2007**. Comparative phytochemical

528   and morphological analyses of three Italian Primula species. *Phytochemistry* **68**: 1683–1691.

529   **Grey-Wilson C**. **1989**. *The genus Dionysia*. Alpine Garden Society.

530   **Gunning BES, Steer MW**. **1996**. *Plant cell biology : structure and function*. Jones and

531   Bartlett Publishers.

532   **Hinterdobler W, Valant-Vetschera KM, Brecker L**. **2017**. New Primula -type Flavones from

533   Exudates of Selected Dionysia spp. (Primulaceae). *Natural Product Communications* **12**:

534   1673–1676.

535   **Jiang N, Doseff AI, Grotewold E**. **2016**. Flavones: From Biosynthesis to Health Benefits.

536   *Plants (Basel, Switzerland)* **5**.

537   **Lidén M**. **2007**. The genus Dionysia (Primulaceae), a synopsis and five new species.

538   *Willdenowia* **37**: 37.

539   **Looker JH, Hanneman WW**. **1962**. Physical and Chemical Properties of Hydroxyflavones. I.

540   Infrared Absorption Spectra of Monohydroxyflavones and Their O-Methyl and O-Acetyl

541   Derivatives 1,2. *The Journal of Organic Chemistry* **27**: 381–389.

542   **Looker JH, Hanneman WW, Kagal SA, Dappen JI, Edman JR**. **1966**. Physical and

543   chemical properties of hydroxyflavones. IV. Infrared absorption spectra of dihydroxyflavones

544   containing the 5-hydroxyl group. *Journal of Heterocyclic Chemistry* **3**: 55–60.

545   **Marinova K, Kleinschmidt K, Weissenböck G, Klein M**. **2007**. Flavonoid biosynthesis in

546   barley primary leaves requires the presence of the vacuole and controls the activity of

547   vacuolar flavonoid transport. *Plant physiology* **144**: 432–44.

548   **Müller H**. **1915**. XCVI.—The occurrence of flavone as the farina of the primula. *J. Chem.*

549   *Soc., Trans.* **107**: 872–878.

550   **Schopker H, Kneisel M, Beerhues L, Robenek H, Wiermann R**. **1995**. Phenylalanine

551   ammonia-lyase and chalcone synthase in glands of Primula kewensis (W. Wats):

552   immunofluorescence and immunogold localization. *Planta* **196**: 712–719.

553   **Sisa M, Bonnet SL, Ferreira D, Van der Westhuizen JH**. **2010**. Photochemistry of

554   Flavonoids. *Molecules* **15**: 5196–5245.

555   **Valant-Vetschera KM, Bhutia TD, Wollenweber E**. **2009**. Exudate Flavonoids of Primula

556   Spp: Structural and Biogenetic Chemodiversity. *Natural Product Communications* **4**: 365–

557   370.

558   **Valant-Vetschera KM, Bhutia TD, Wollenweber E**. **2010**. Chemodiversity of exudate

559   flavonoids in Dionysia (Primulaceae): A comparative study. *Phytochemistry* **71**: 937–947.

560   **Vitalini S, Flamini G, Valaguzza A, Rodondi G, Iriti M, Fico G**. **2011**. Primula spectabilis

561   Tratt. aerial parts: Morphology, volatile compounds and flavonoids. *Phytochemistry* **72**:

562   1371–1378.

563   **Wendelbo P**. **1971**. On xeromorphic adaptations in the genus Dionysia (Primulaceae). *Ann*

564   *Naturhist Mus Wien* **75**: 249–254.

565   **Wightman R, Busse-Wicher M, Dupree P**. **2019**. Correlative FLIM-confocal-Raman

566   mapping applied to plant lignin composition and autofluorescence. *Micron* **126**: 102733.

567   **Wightman R, Wallis S, Aston P**. **2018**. Leaf margin organisation and the existence of

568   vaterite-producing hydathodes in the alpine plant Saxifraga scardica. *Flora* **241**: 27–34.

569   **Wollenweber E, Schnepf E**. **1970**. Vergleichende Untersuchungen über die flavonoiden

570   Exkrete von "Mehl"- und "Öl" -Drüsen bei Primeln und die Feinstruktur der Drüsenzellen. *Z.*

571   *Pflanzenphysiol* **62**: 216–227.

572

573

574

575   **Supplementary Data list.**

576

577   **Dataset S1 comprising Figures S1-S7 and Table S1.** All data and interpretations/

578   commentary for HLPC, LCMS, HMRS and NMR chemical analyses.

579

580   **Figure S8**.

581

582   **Figure S9**.

583
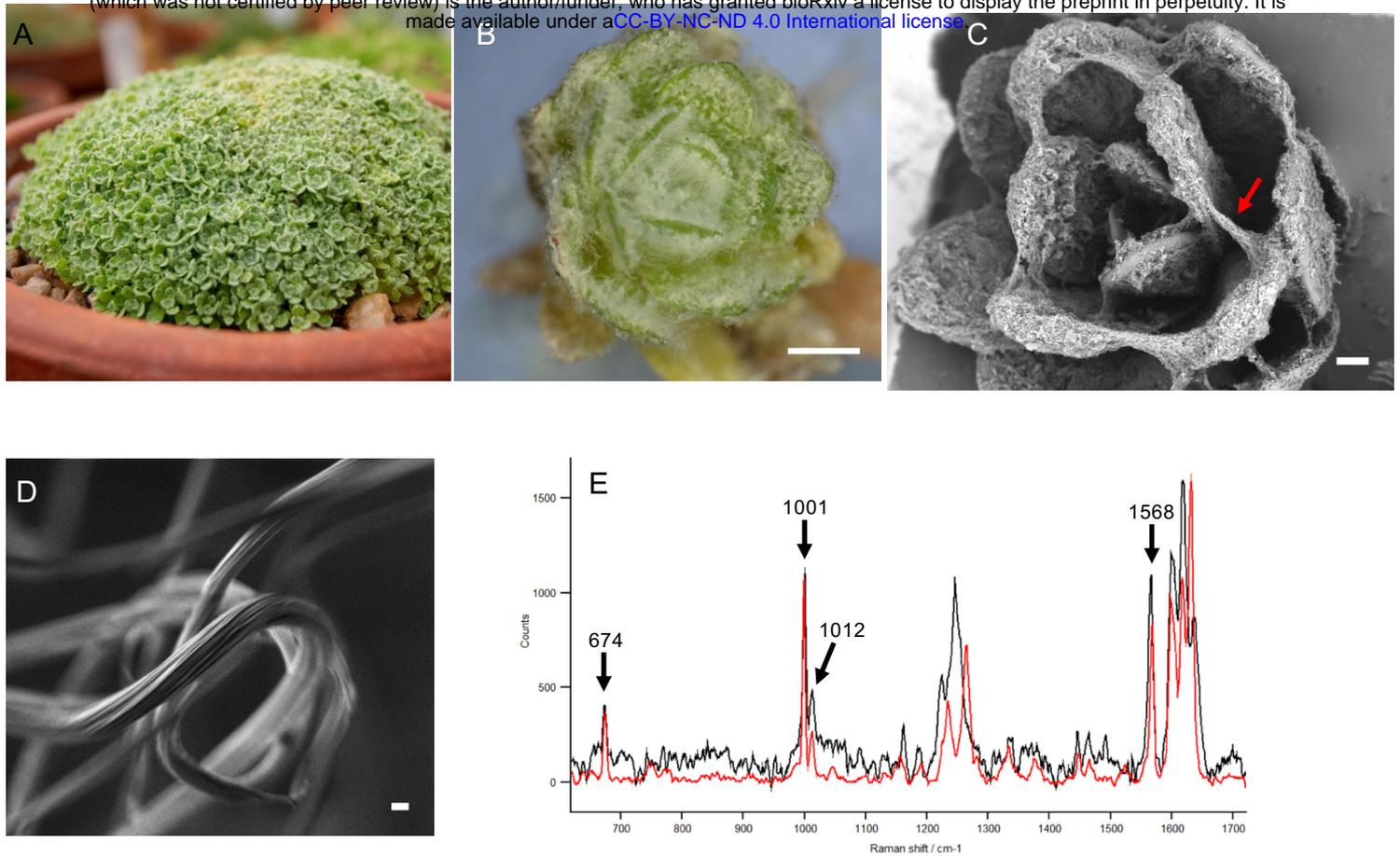
Figure 1. Farina wool observations on leaves of *Dionysia tapetodes.* A) Overview of the densely-packed, cushion-forming *D. tapetodes*. B) Stereomicroscope image of white wooly farina on leaves of *D. tapetodes.* Scale bar = 1 mm. C) Scanning electron microscopy (SEM) of wooly farina distributed on and between leaves (e.g. red arrow) of *D. tapetodes*. Scale bar = 300 μm. D) High magnification SEM image of farina fibre showing fine surface structure. Scale bar = 1 μm. E) Raman microscopy of fingerprint region of farina of *Dionysia tapetodes* (black) compared with that of the powdery farina from *Primula marginata* (red). Principle peak assignments (cm⁻¹) common to both types of farina are indicated.
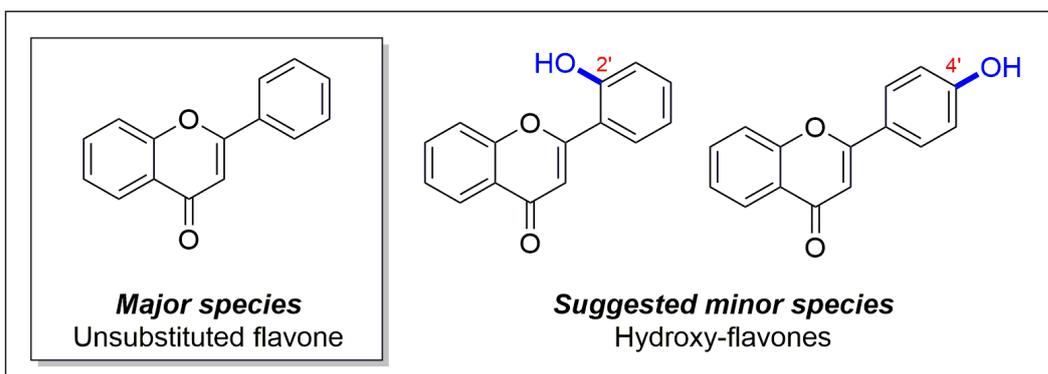
Figure 2. Molecular structures of candidate molecular species that form the wooly farina of *D. tapetodes*. Structures are derived from chemical analyses described in dataset S1.
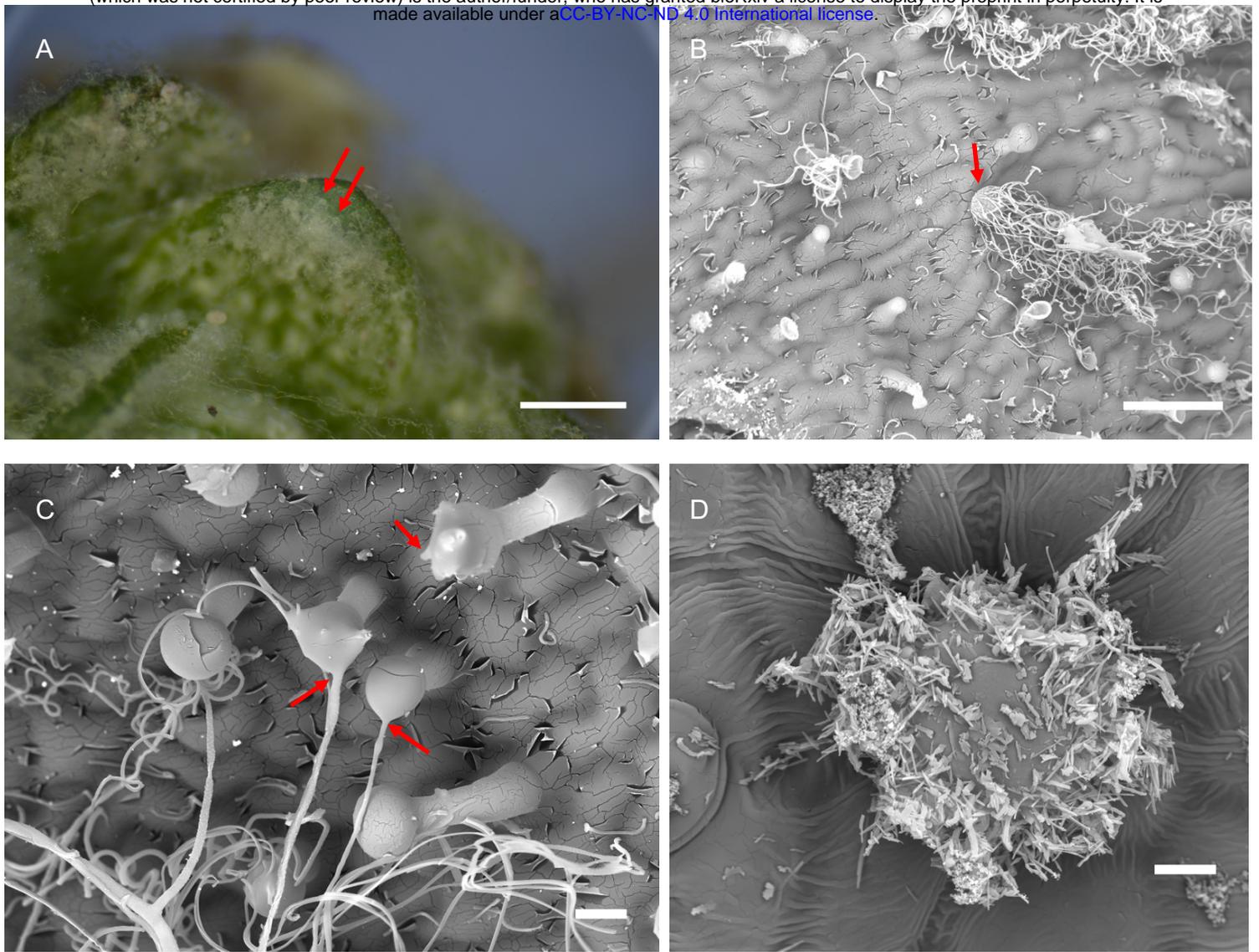
Figure 3. Formation of farina at the single cell level. A) Stereomicroscope image showing examples of wool exit points (red arrows) on the surface of the leaf of *D. tapetodes.* Scale bar = 500 μm. B) SEM image of glandular trichomes, including an example of a mature glandular trichome producing large quantities of wooly farina (red arrow). Scale bar = 50 μm. C) SEM image showing farina wool exit points (red arrows) from glandular trichomes. Scale bar = 10 μm. D) SEM image showing glandular trichome of *P. marginata* covered with powdery flavone farina. Scale bar = 10 μm.
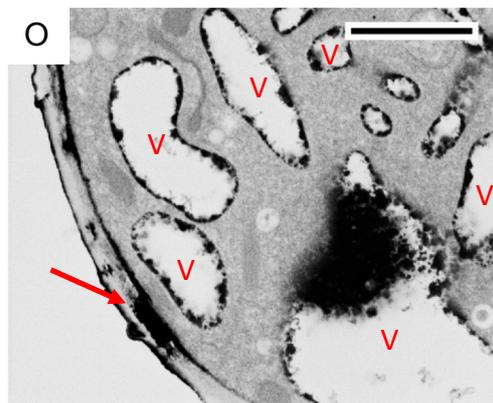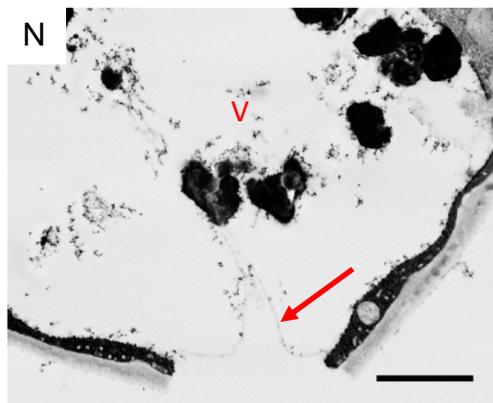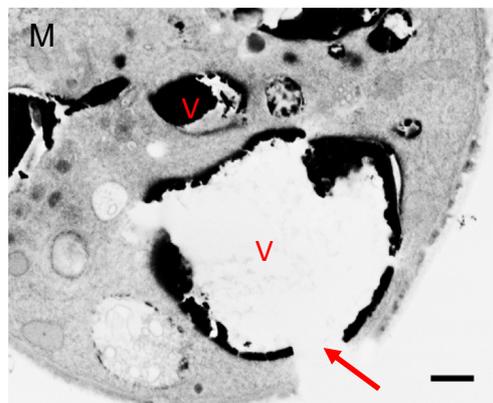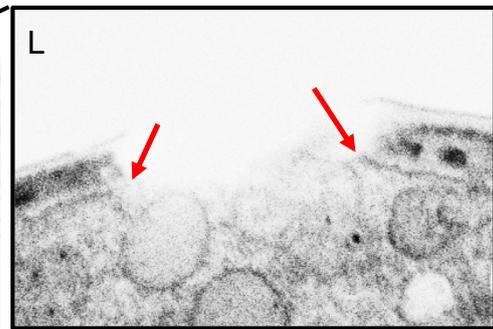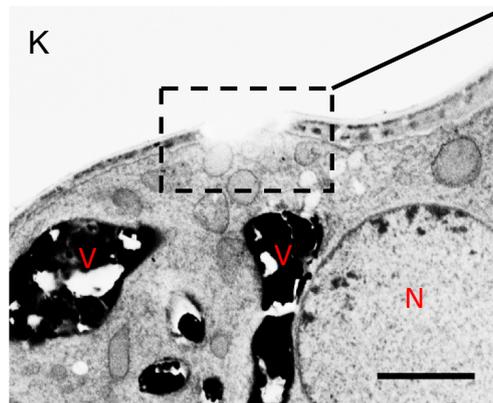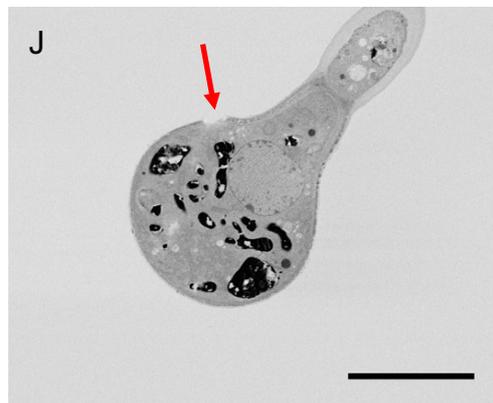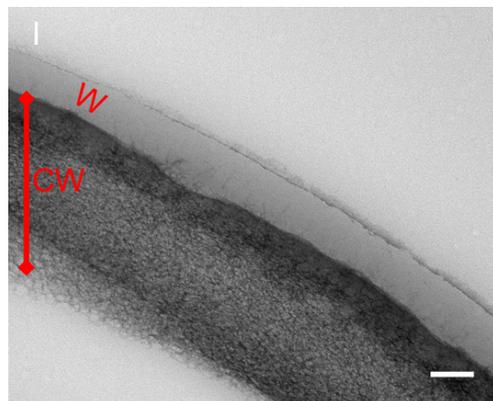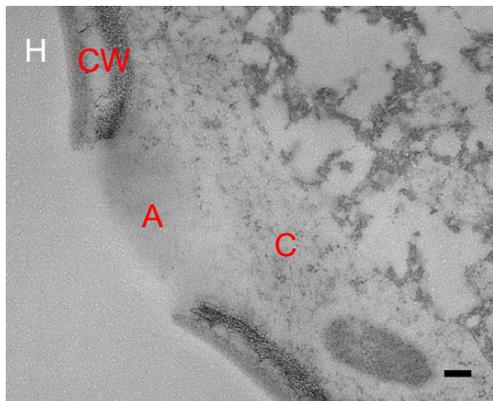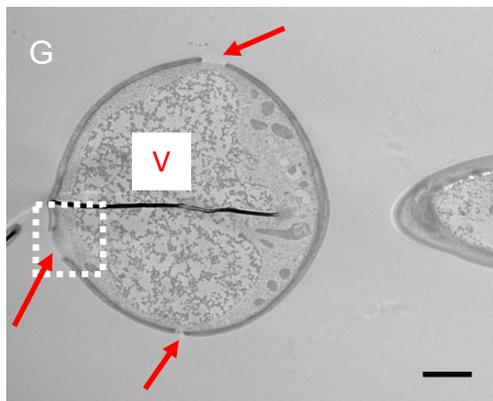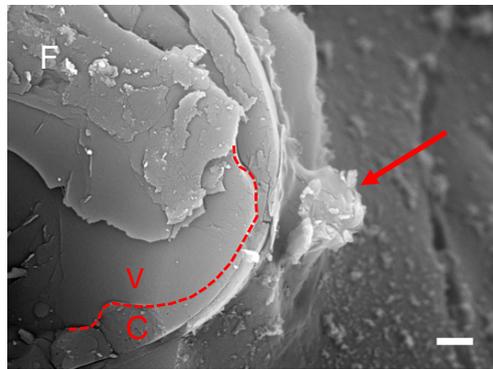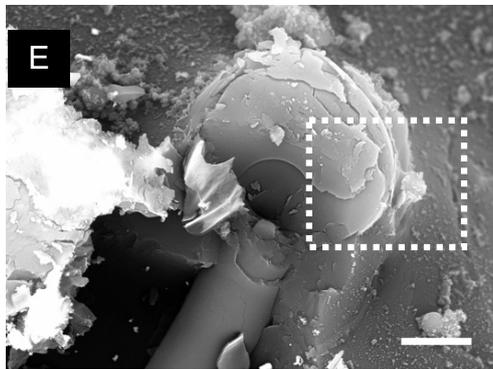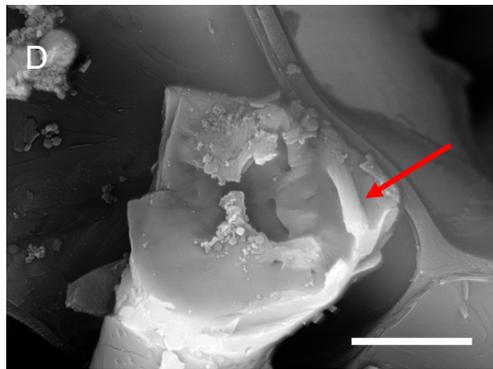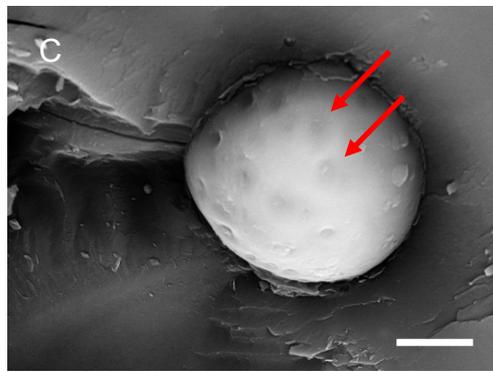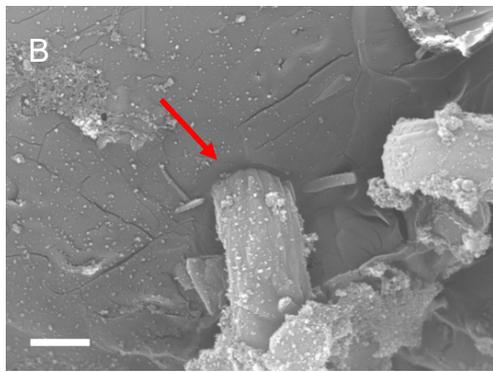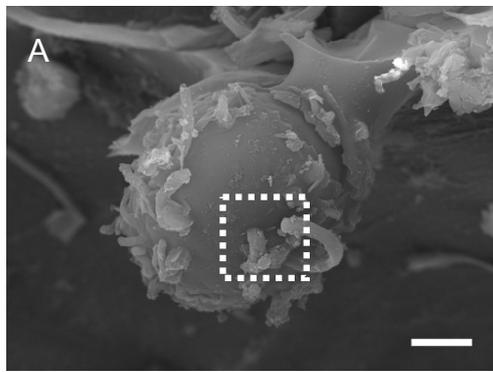
Figure 4. Exit points of farina wool from glandular trichomes. A) SEM image showing wool exiting from the surface of a glandular trichome cell. A magnified view of the boxed region is shown in (B). Cell surface-farina interface is labeled by a red arrow. Bars = 5 μm (A) and 1 μm (B). C) Surface of glandular trichome cell after ethanol wash to remove farinose material. Examples of wool exit points are labeled by red arrows. Bar = 5 μm. D) SEM after cryo-fracture showing inner face of part of the surface of a trichome cell. A piece of farina wool is found to be present intact inside the cell (red arrow). Bar = 5 μm. E) SEM after cryofracture revealing cell contents. Bar = 5 μm. A magnified view of the boxed area is shown in (F) where wool exit is observed (red arrow). The dashed line represents the location of the tonoplast. V= Vacuole, C= cytoplasm. The Vacuole is seen to be in close proximity to the wool exit site. Bar = 1 μm. G) Transmission EM (TEM) image of section through glandular trichome. Wool exit sites are marked by red arrows and are defined as a gap in the cell wall. Electron dense material, consistent with vacuole contents (V), are in close proximity to these sites. Dark line in the centre is an artefact from a fold in the section. Bar = 2 μm. H) a magnified view of a wool exit site (boxed region) showing a gap in the cell wall (CW) and an amorphous region (A) within this gap. Beneath the amorphous region is observed a small amount of cytoplasm (C). Bar = 200 nm. (I) TEM image of a section of intact cell wall (CW) overlayed by a waxy low density layer (W). Bar = 100 nm. J, K, L) FE-SEM of glandular head showing wool exit site (arrow in J) Bar = 10 μm. A magnified view of the area covering the exits site is shown in (K) together with the electron dense vacuoles (V) and the Nucleus (N) Bar = 2 μm. Further magnification (L) shows the plasma membrane does not traverse the gap (arrows). M, N) Exit sites that extend to the vacuole. In (N) the tonoplast is found to be intact (arrow). Bars = 2 μm. O) A build up of electron dense material accumulates within a void in the cell wall (arrow). Vacuoles (V) containing similar electron dense material are found in close proximity. Bar = 2 μm.
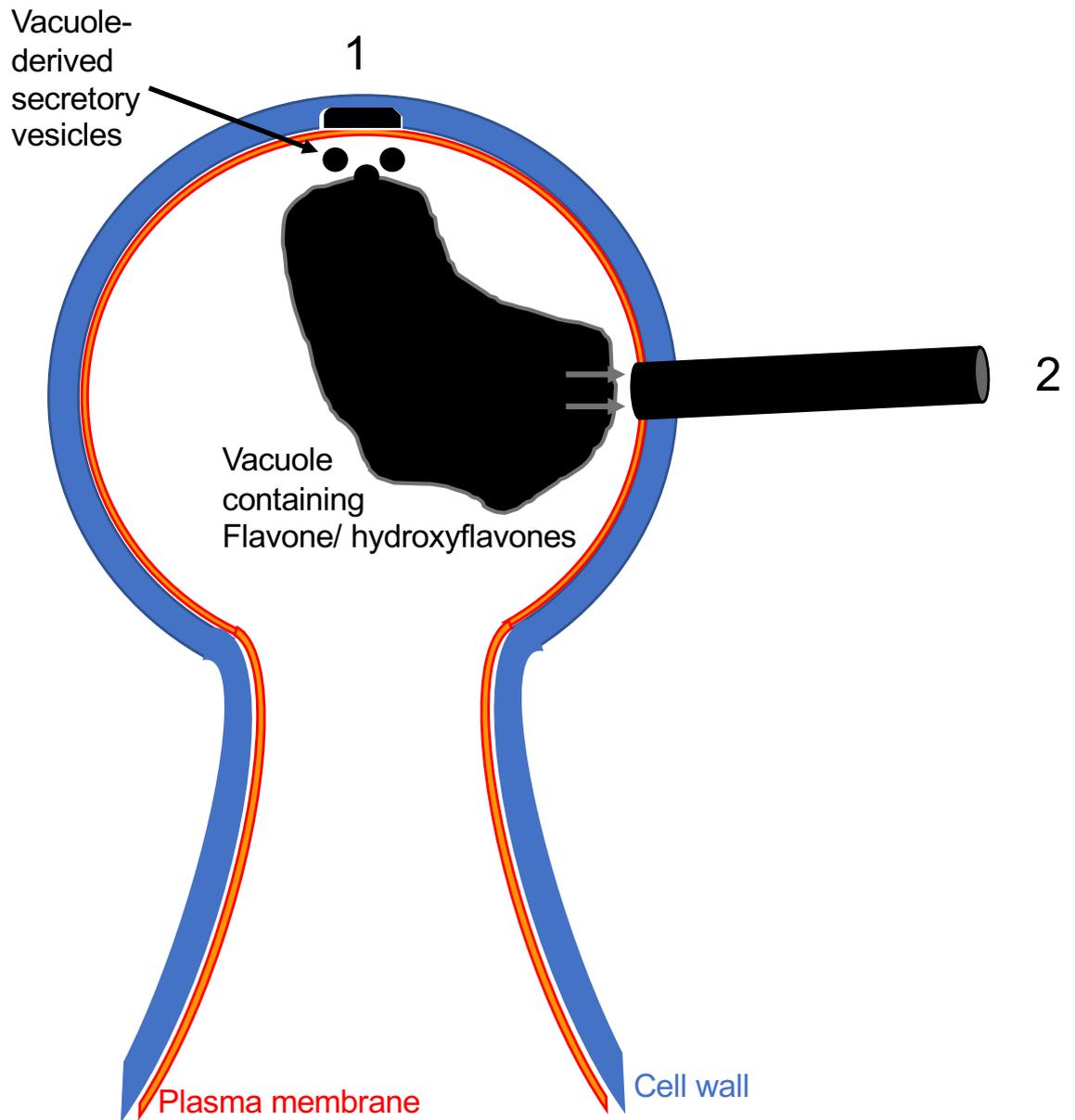
Figure 5 – Proposed schematic of farina wool formation by the glandular trichome. (1) Localised cell wall digestion commences from the membrane face and is coupled with deposition of (hydroxy)flavones within the space. (2) Cell wall digestion produces a hole through which the (hydroxy)flavones are extruded. The (hydroxy)flavones may be deposited directly from the vacuole.

Dataset S1 including Figures_S1_to_S7_and Table S1

Analytical HPLC analysis of wool fibre samples

To assess the purity of the sample, HPLC analysis was performed using two different gradients (5-95% and 40-95% acetonitrile in water) to ensure that all peaks present were observed.
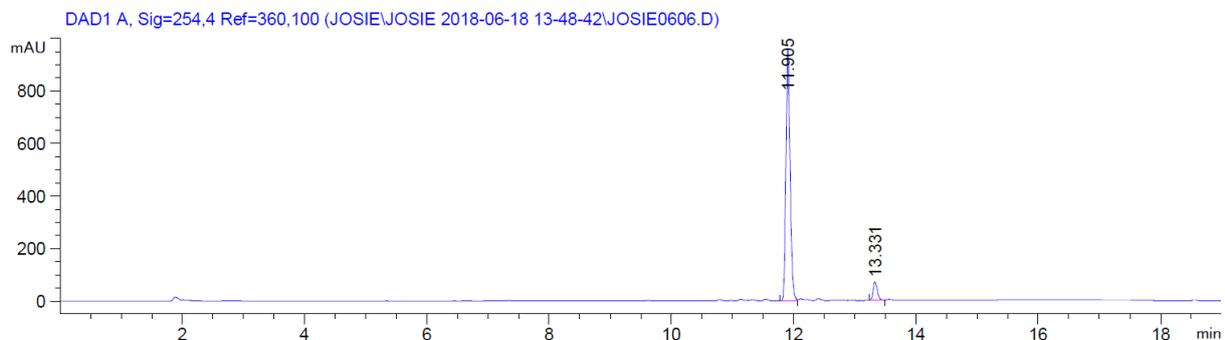
Figure S1a The HPLC spectra for analysis of the sample using a 5-95% acetonitrile in water gradient. The large signal at 2-2.5 minutes in the 220 nm trace (Figure 1 and 2) is due to dimethylsulfoxide (DMSO) which was used to dissolve the sample.
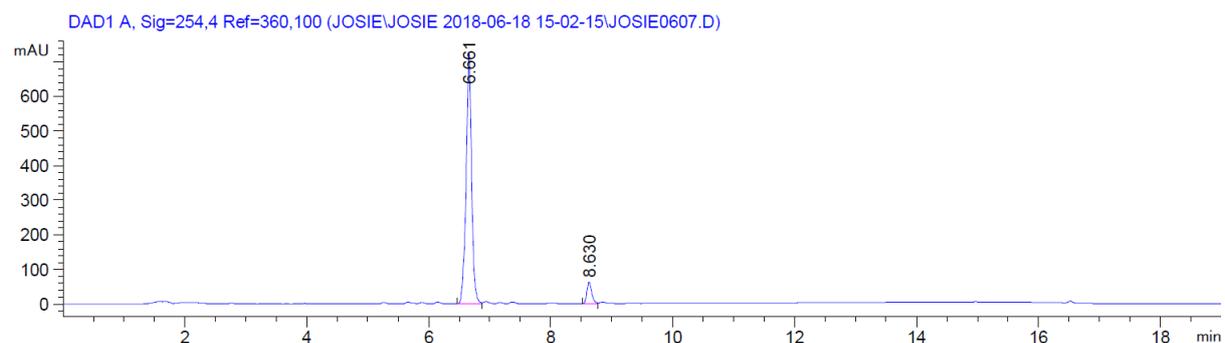
Figure S1b The HPLC spectra for analysis of the sample using a 5-95% acetonitrile in water gradient.

Table S1 The peaks observed in the spectra shown in Figure 1.

Peak	Retention time (min)	Area (mAU*s)	Area (%)
1	11.905	4507.078	93.0
2	13.331	340.296	7.0
1	6.661	4535.346	93.0
2	8.630	339.714	7.0

S2: Mass spectrometry of wool fibre sample
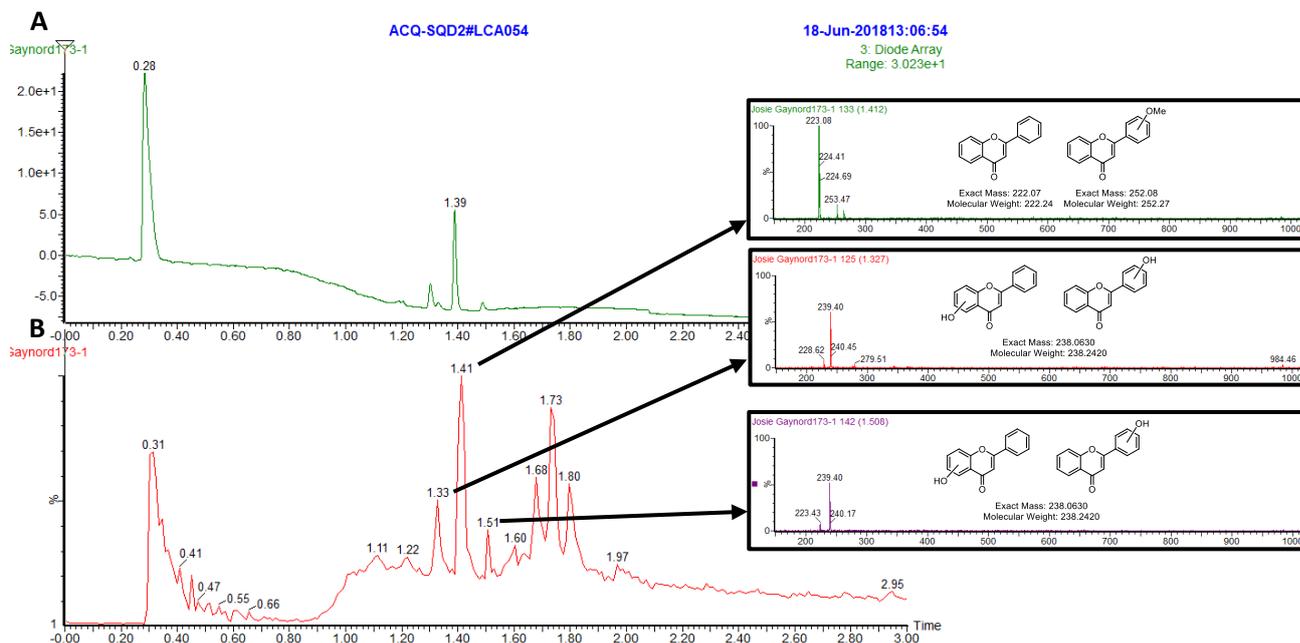
Figure S2a A: The UV trace for the LCMS spectrum of the plant sample. B: The corresponding ES+ trace. Insets are mass traces (ES+) for individual peaks, as indicated by the arrows. Suggested chemical structures with exact masses and molecular weights are shown over the relevant mass spectra.
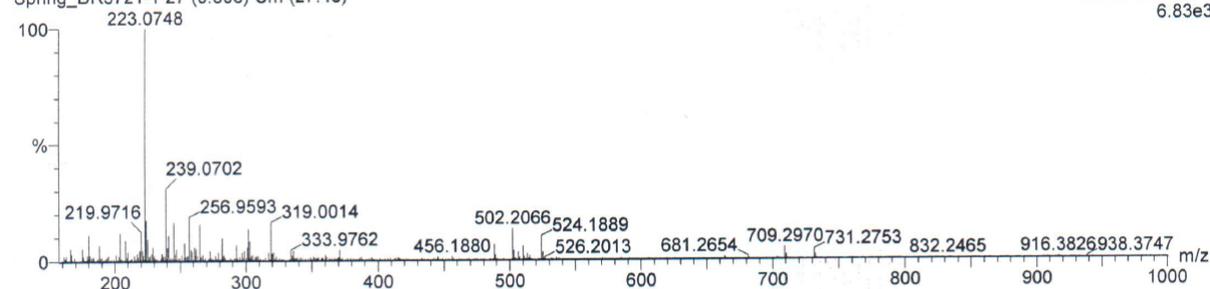
Figure S3 The high-resolution mass spectrum (HRMS) for the plant sample.

HPLC analysis of pure flavone
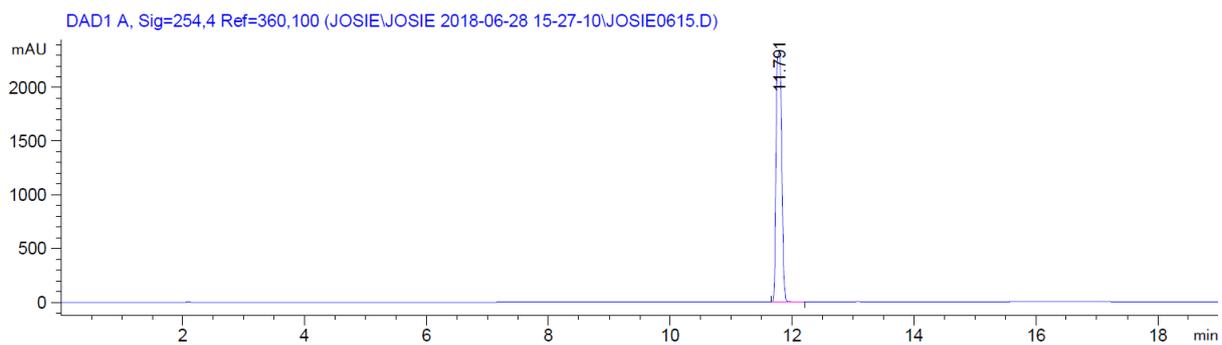
Figure S4 The HPLC spectra for analysis of pure Flavone using a 5-95% acetonitrile in water gradient.

NMR comparison of commercially-available flavone and wool fibre
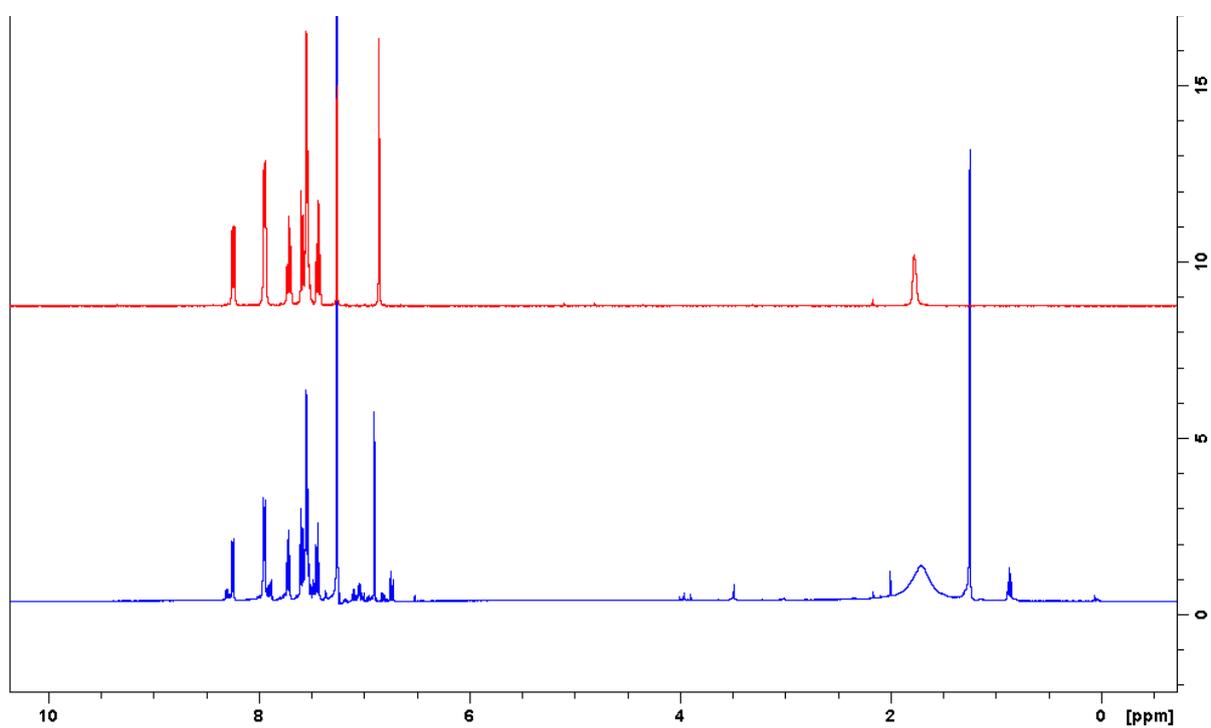
Figure S5a A comparison of the ^{1}H NMR spectra for a pure sample of flavone (red) and the wool fibre sample (blue) between 10 and 0 ppm.
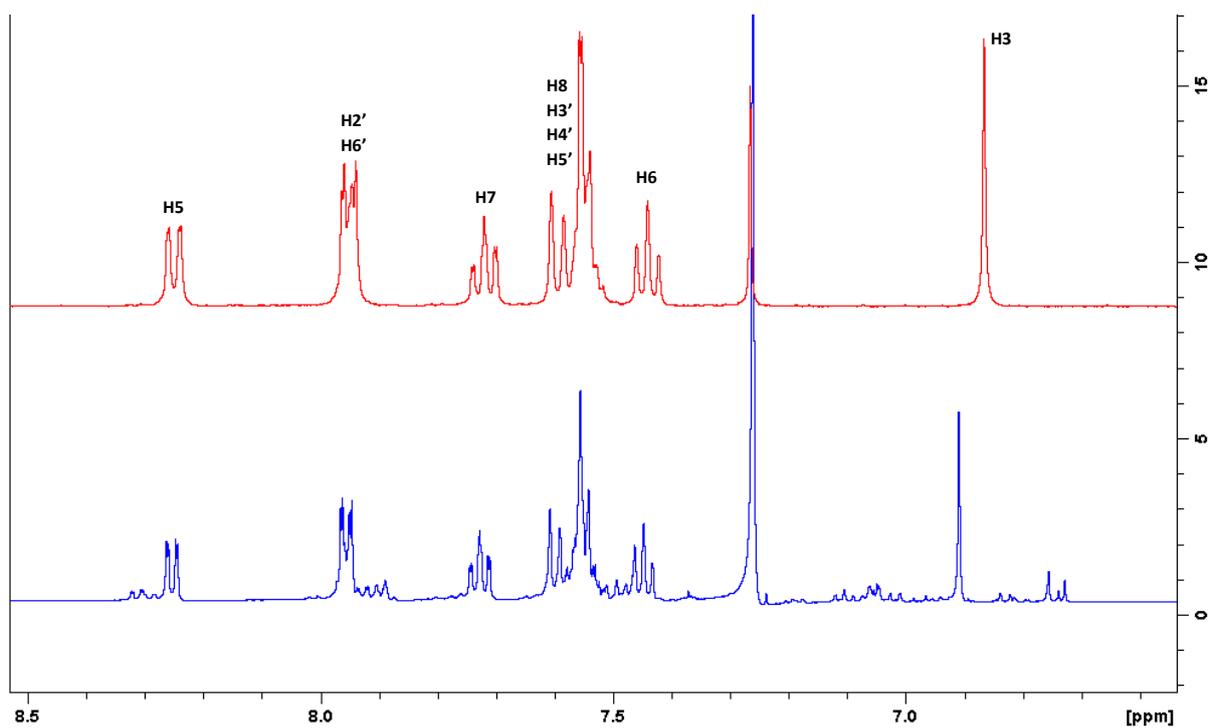
Figure S5b A comparison of the ^{1}H NMR spectra for a pure sample of flavone (red) and the wool fibre sample (blue) between 8.5 and 6.5 ppm.
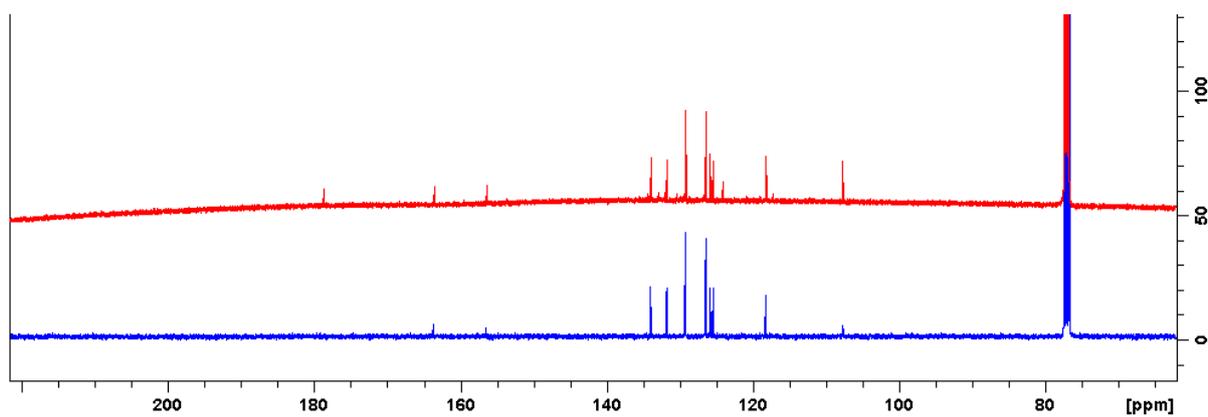
Figure S5c A comparison of the ^{13}C NMR between 220 and 70 ppm for a pure sample of flavone (red) and the wool fibre sample (blue).

NMR Analysis of wool fibre sample

The sample was analysed using the following NMR experiments: ^{1}H NMR (Figure S6a), ^{13}C NMR (Figure S6b), DEPT 135 (Figure S6c), COSY (Figure S6d), HSQC (Figure S6e) and HMBC (Figure S6f).

The ^{1}H and ^{13}C NMR of pure flavone were compared to the plant sample and the signals were found to match (S5), providing further evidence that the major component of the plant sample mixture is unsubstituted flavone. The NMR assignments are therefore as follows[1,2]:

^{1}H NMR (500 MHz, CDCl$_3$) δ 8.26-8.24 (m, 1H, H5), 7.96-7.94 (m, 2H, H2', H6'), 7.74-7.71 (m, 1H, H7), 7.60-7.51 (m, 4H, H8, H3', H4', H5'), 7.46-7.43 (m, 1H, H6), 6.91 (s, 1H, H3)

^{13}C NMR (125 MHz, CDCl$_3$) δ 178.7 (C, C4), 163.6 (C, C2), 156.5 (C, C9), 134.0 (CH, C7), 131.9 (C, C1'), 131.8 (CH, C3', C5'), 129.2 (CH, C4'), 126.5 (CH, C2', C6'), 125.9 (CH, C5), 125.4 (CH, C6), 124.1 (C, C10), 118.3 (CH, C8), 107.8 (CH, C3)
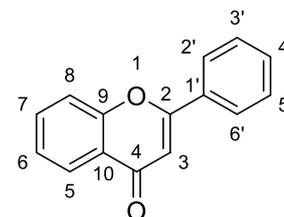
[1] B.-H. Moon, Y. Lee, C. Shin, Y. Lim, Complete Assignments of the ^{1}H and ^{13}C NMR Data of Flavone Derivatives, *Bull. Korean Chem. Soc.* **26** (4), 603-608 (2005)
[2] D. W. Aksnes, A. Standnes, Ø. M. Andersen, Complete Assignment of the ^{1}H and ^{13}C NMR Spectra of Flavone and its A-Ring Hydroxyl Derivatives, *Magnetic Resonance in Chemistry* **34**, 820-823 (1996)
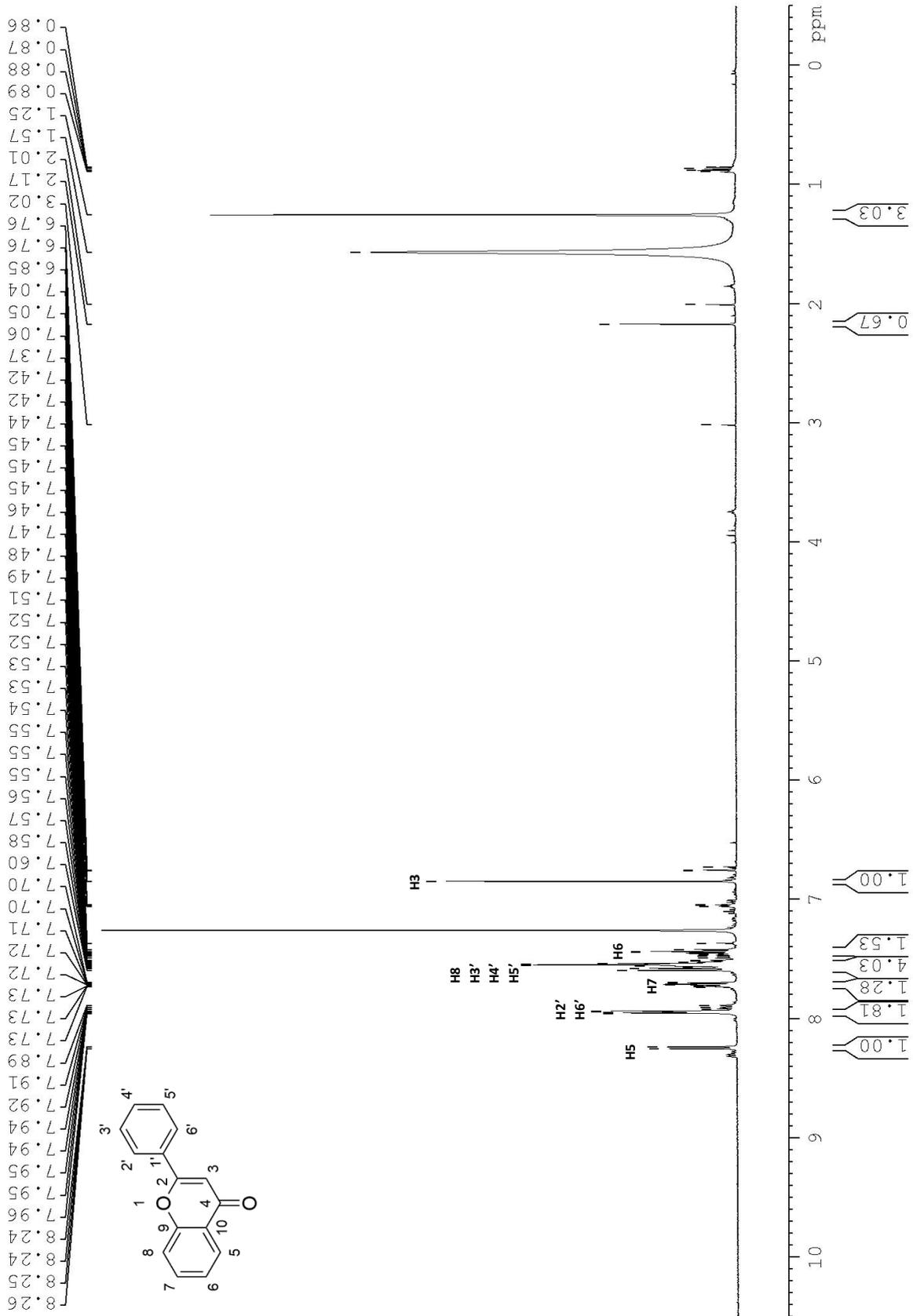
Figure S6a The assigned ¹H NMR spectrum of the plant sample.
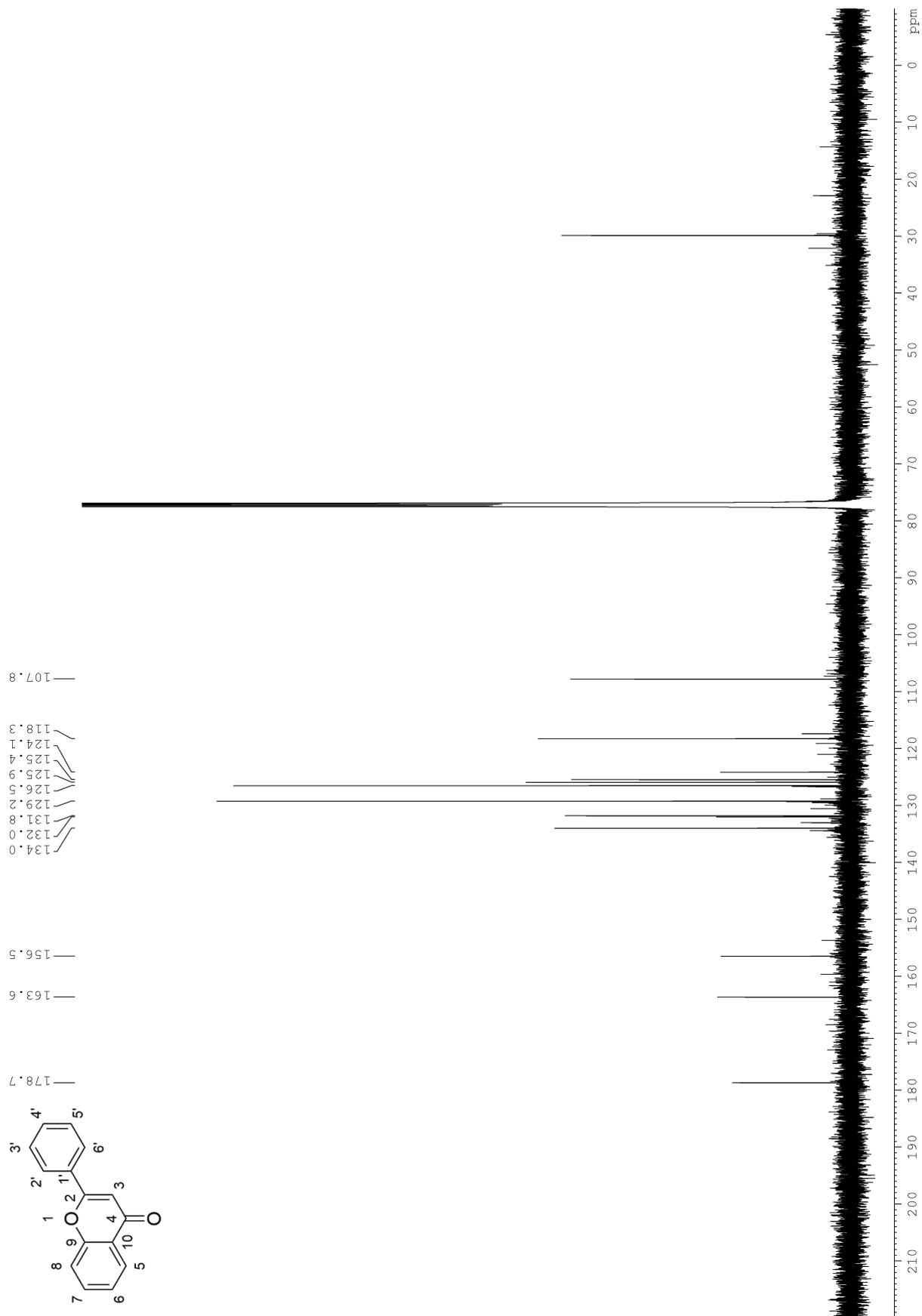
Figure S6b The ^{13}C NMR spectrum of the plant sample
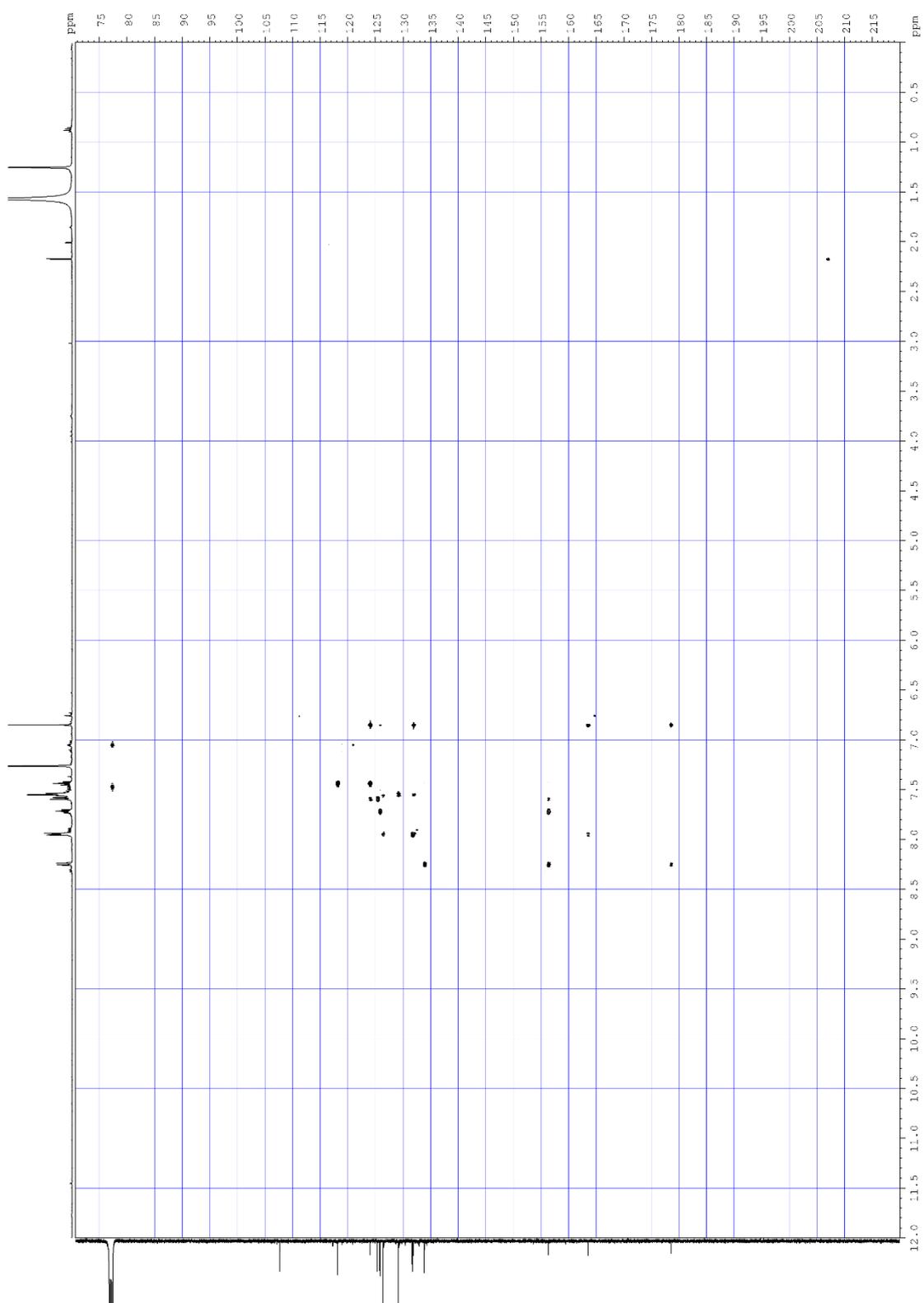
Figure S6c The HMBC spectrum of the plant sample
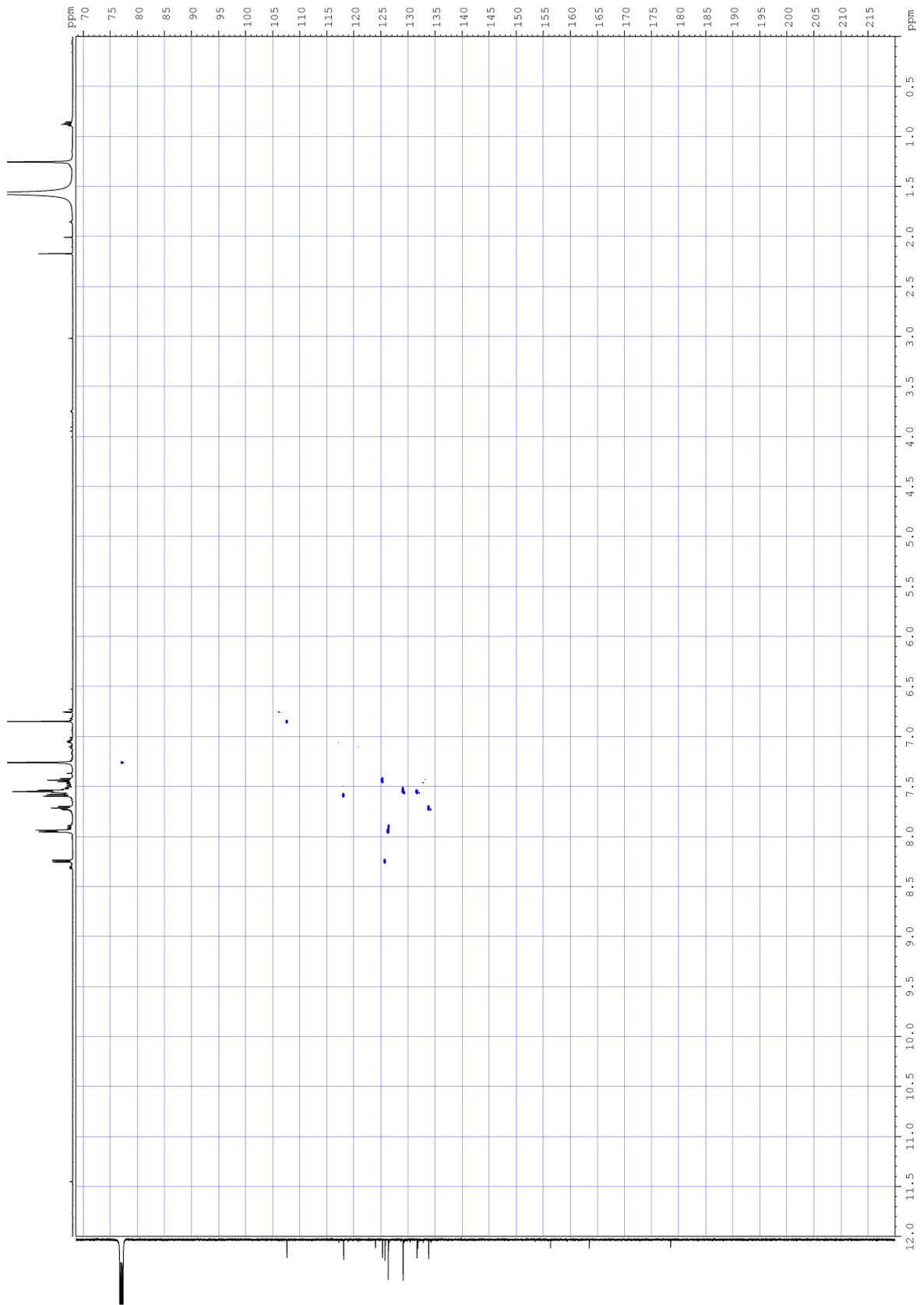
Figure S6d The HSQC spectrum of the plant sample
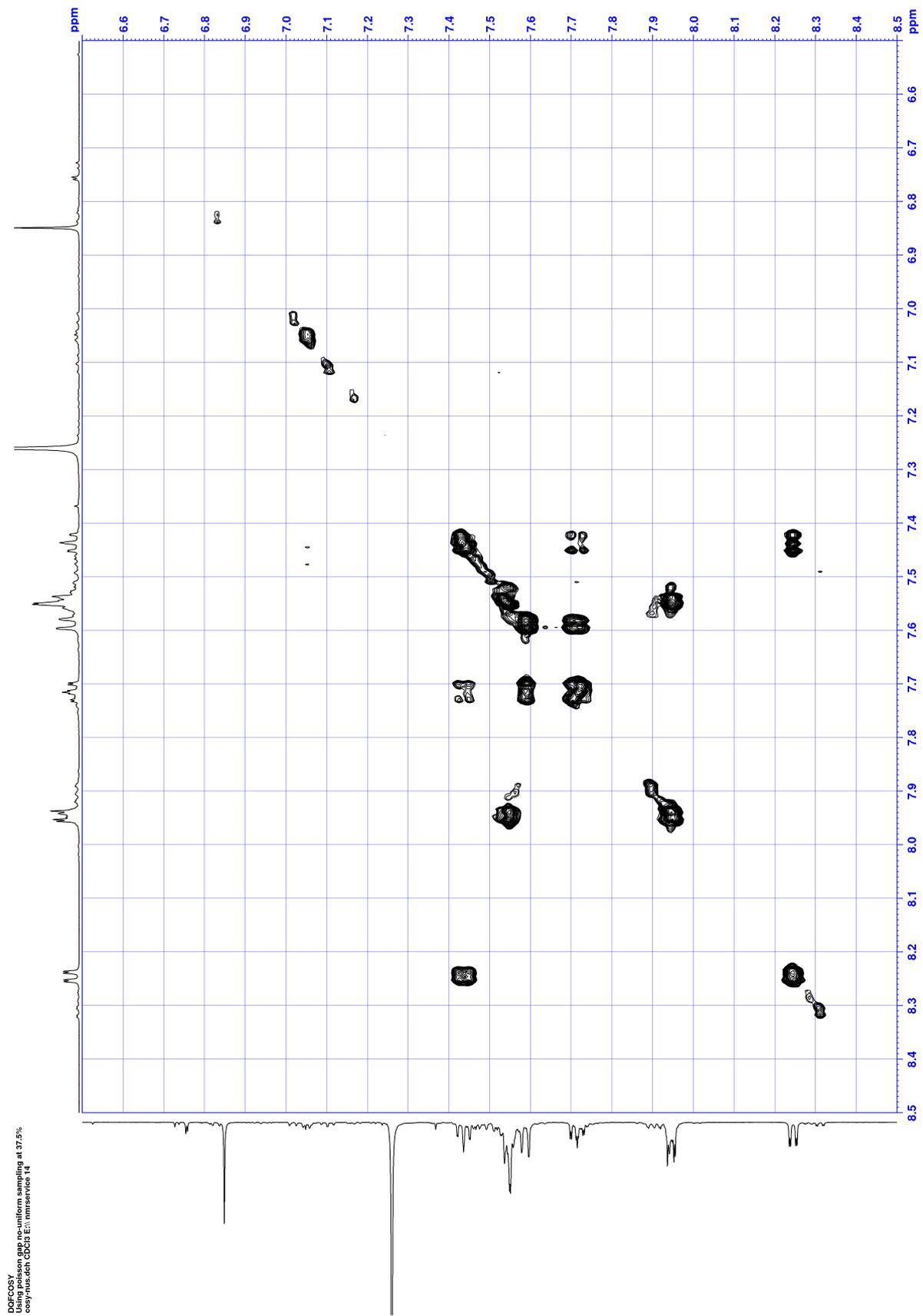
Figure S6e The COSY spectrum of the plant sample
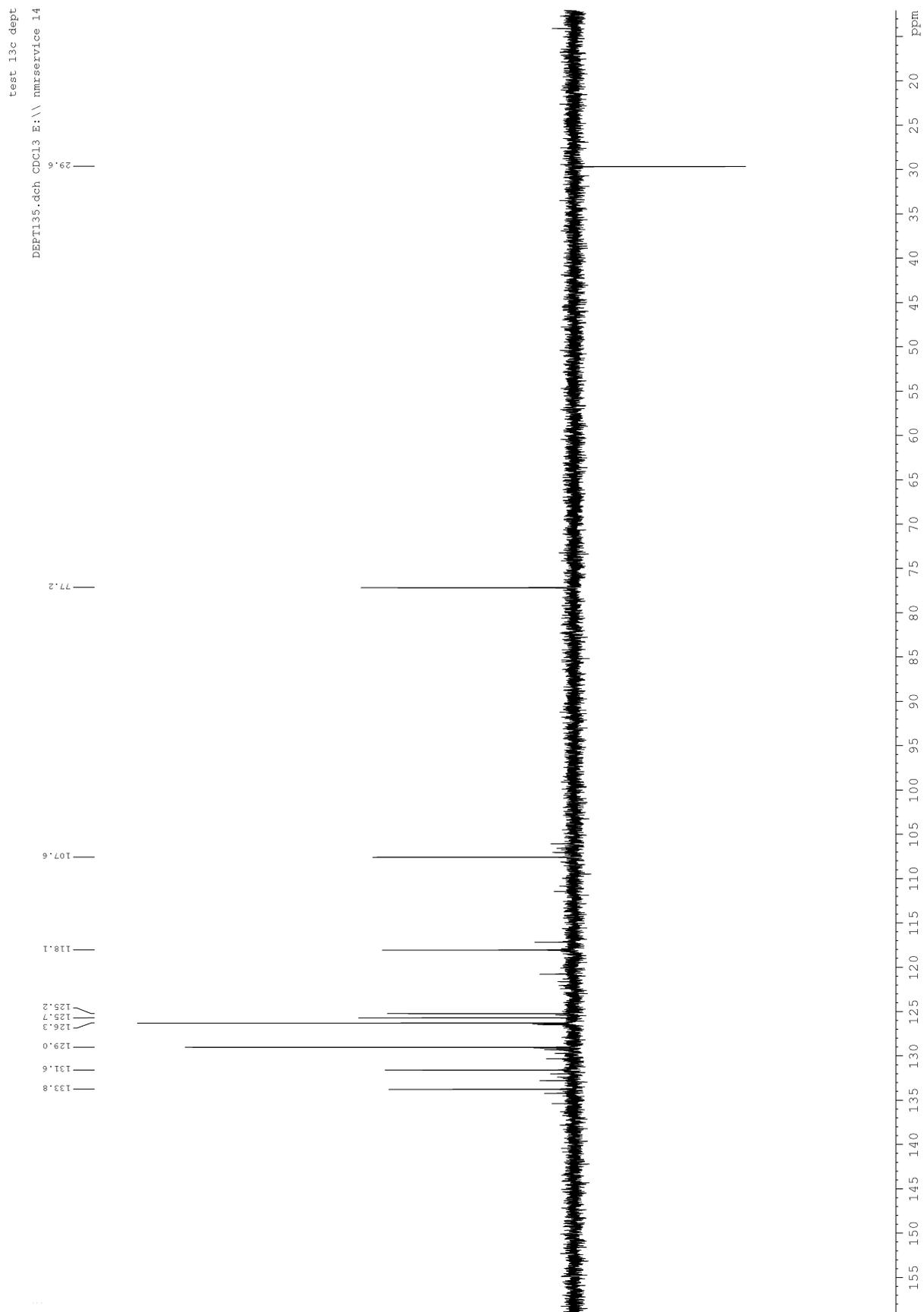
Figure S6f The DEPT 135 spectrum of the plant sample

2D NMR experiments to investigate substitution patterns on flavones

To investigate the structure of the minor species present in the wooly farina sample, a HSQC experiment was run with non-uniform sampling to increase the resolution of the spectrum (Figures S7a and S7b).
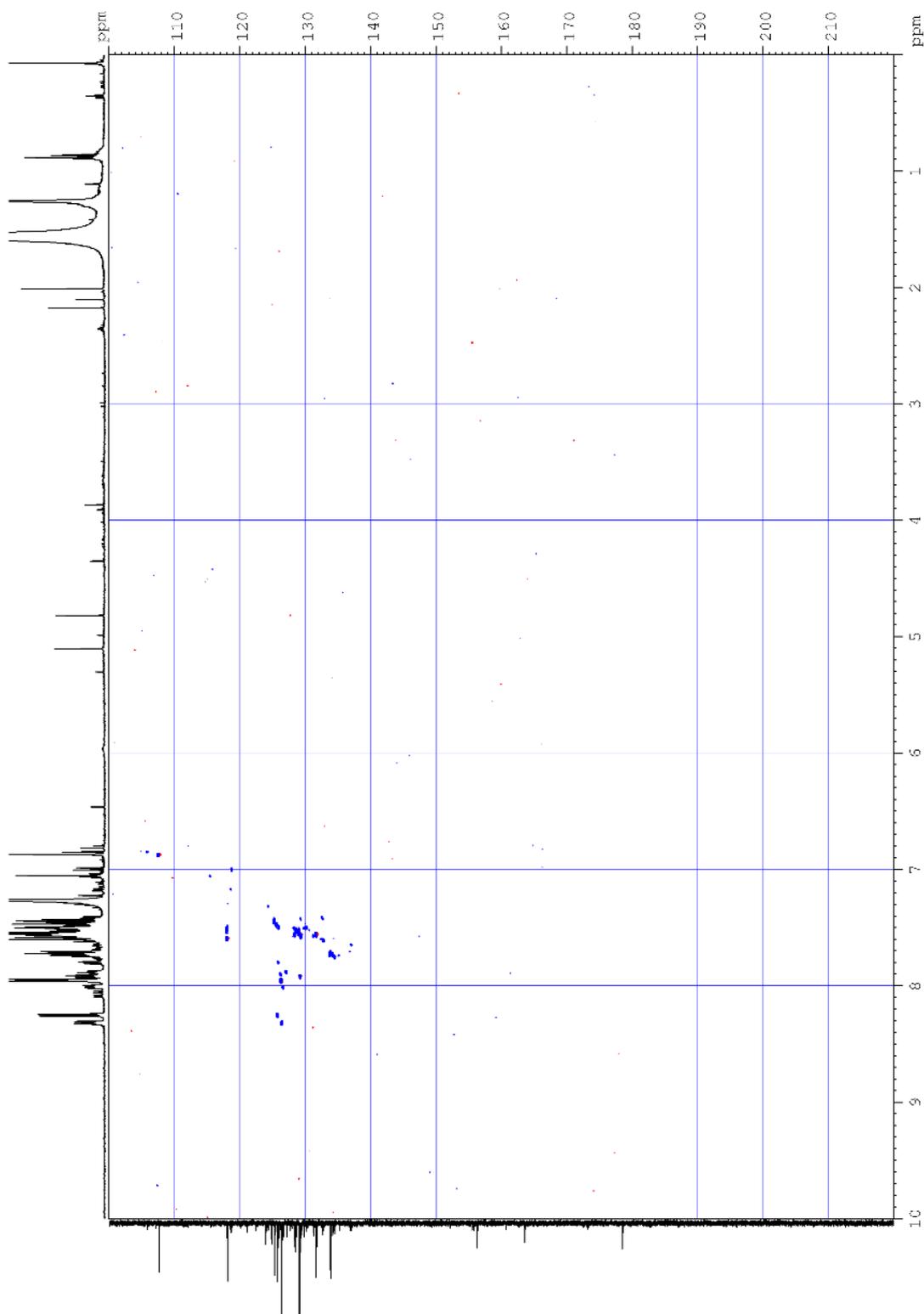
Figure S7a The spectrum of the HSQC experiment (run with non-uniform sampling).
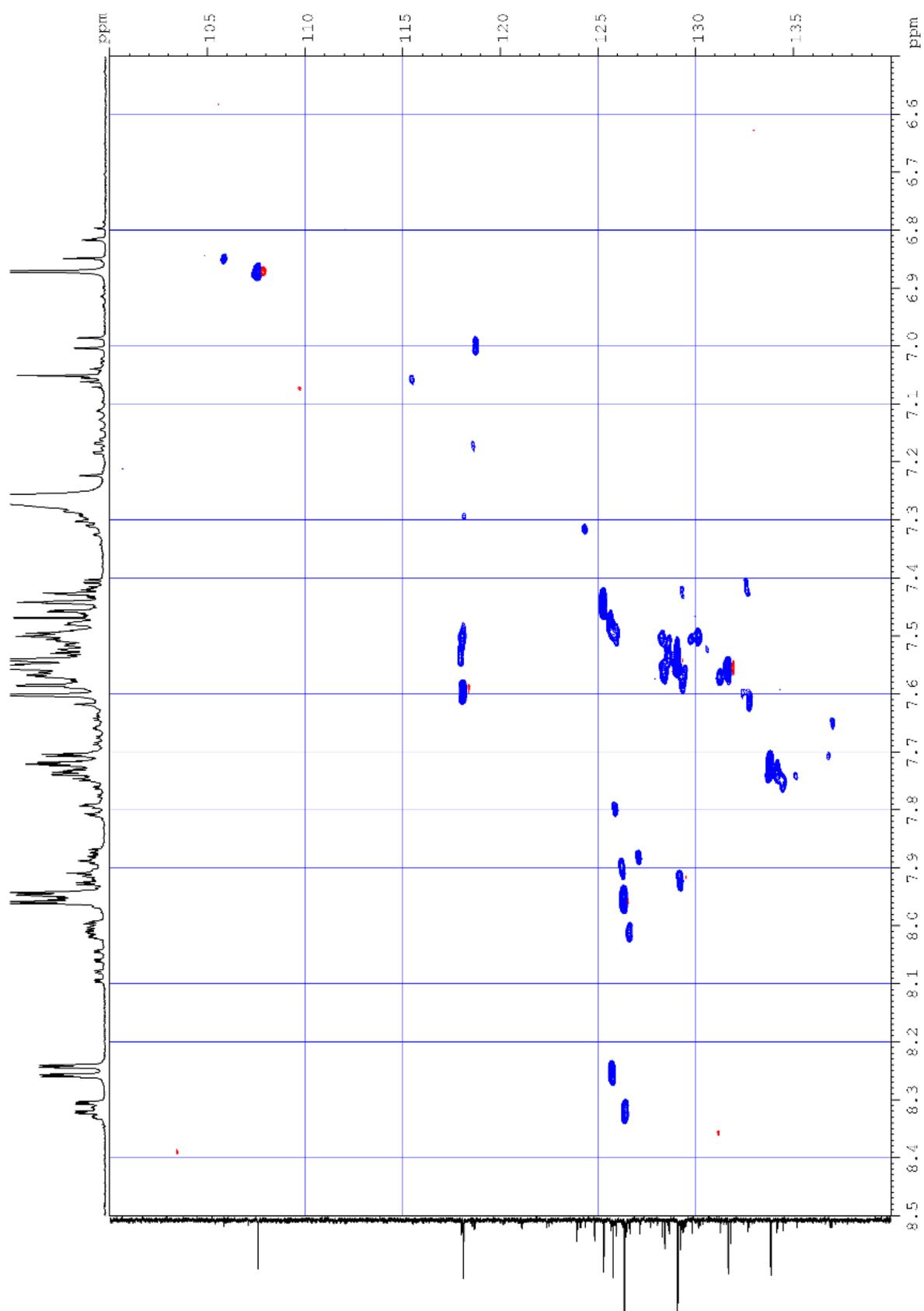
Figure S7b A zoomed in section of the aromatic region of the HSQC experiment (run with non-uniform sampling).

Without NMR, LCMS, HRMS and HPLC analysis of the isolated components of the plant sample mixture, the structure of the minor species cannot be stated with 100% confidence. However with the data from the LCMS, HPLC, HRMS and NMR, suggestions can be made.

The masses from the LCMS indicated that mono-hydroxy or mono-methoxyflavones were present in the wooly farina sample. Literature values for carbon atoms bearing a hydroxy or methoxy substituent in flavones are very similar and signals are present at 3.9-4.0 ppm in the ^{1}H NMR spectrum which could correlate to the methyl group of a methoxy substituent, however with the NMR data available it could not be confirmed if methoxy-substituted flavones were present.

For hydroxy substitution, each potential substitution site was considered in turn. The expected shifts of the protons and carbons with hydroxy-substitution were based on literature values[3,4]. From the information provided by the HSQC experiment, the most likely substitution pattern is 4'-hydroxyflavone:
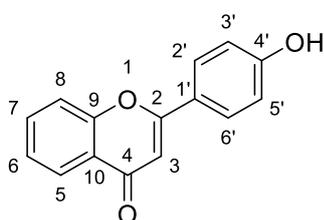
The evidence for this is as follows:

A signal is present in the ^{13}C NMR spectrum at 160.7 ppm which is in the correct region for the quaternary C4' carbon with either a hydroxyl substitution (Figure S7c).

Correlation is observed in the HSQC between a ^{13}C signal at 127.1 ppm and a ^{1}H signal at 7.88 ppm (A, Figure S7d). These match the expected shifts for an aromatic CH in a meta position to the hydroxylation site (i.e. the CH at either C2' or C6').

Correlation is observed between a ^{13}C signal at 118.6 ppm and a ^{1}H signal at 7.16 ppm (B, Figure S7d) which match the expected shifts for an aromatic CH in an ortho position relative to the hydroxyl group (i.e. the CH at C3' or C5').

[3] D. H. Williams, I. Flemming, *Spectroscopic Methods in Organic Chemistry* (McGraw-Hill Companies, ed. 5, 1996)
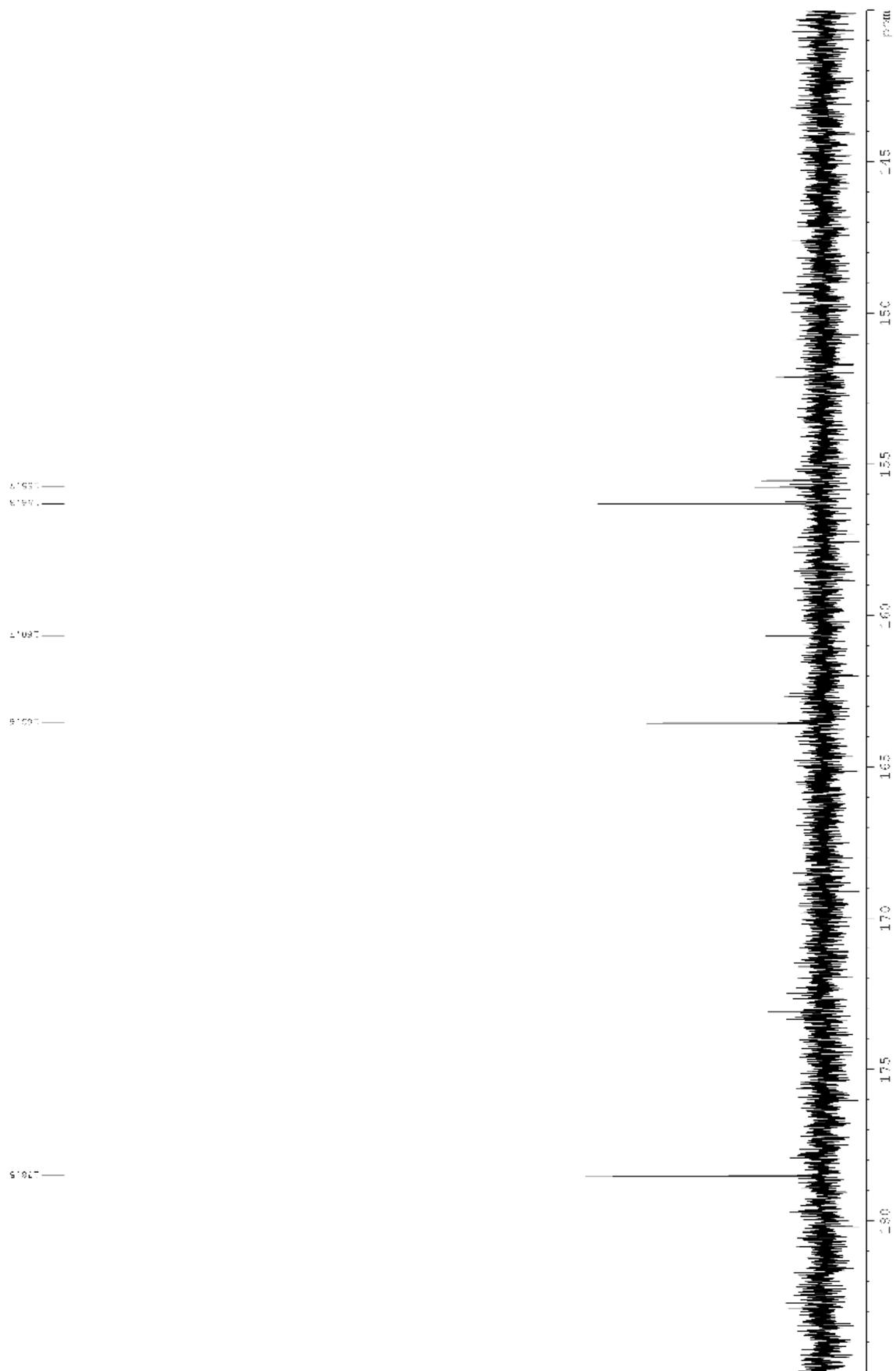[4] Y. Park, B.-H. Moon, E. Lee, Y. Lee, Y. Yoon, J.-H. Ahn, Y. Lim, *Magn. Reson. Chem*. **45**, 674–679 (2007)

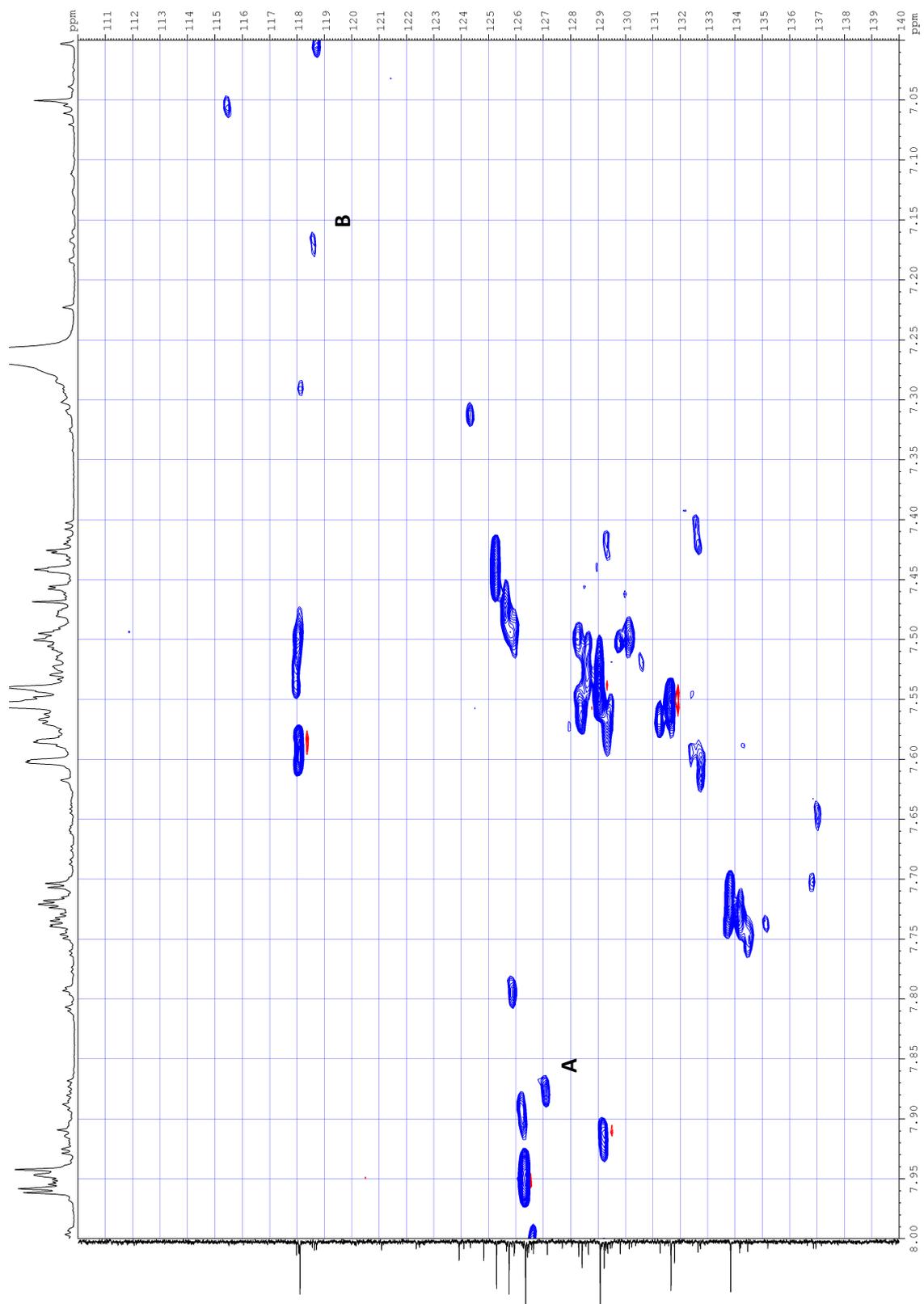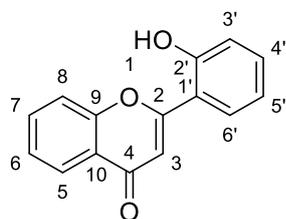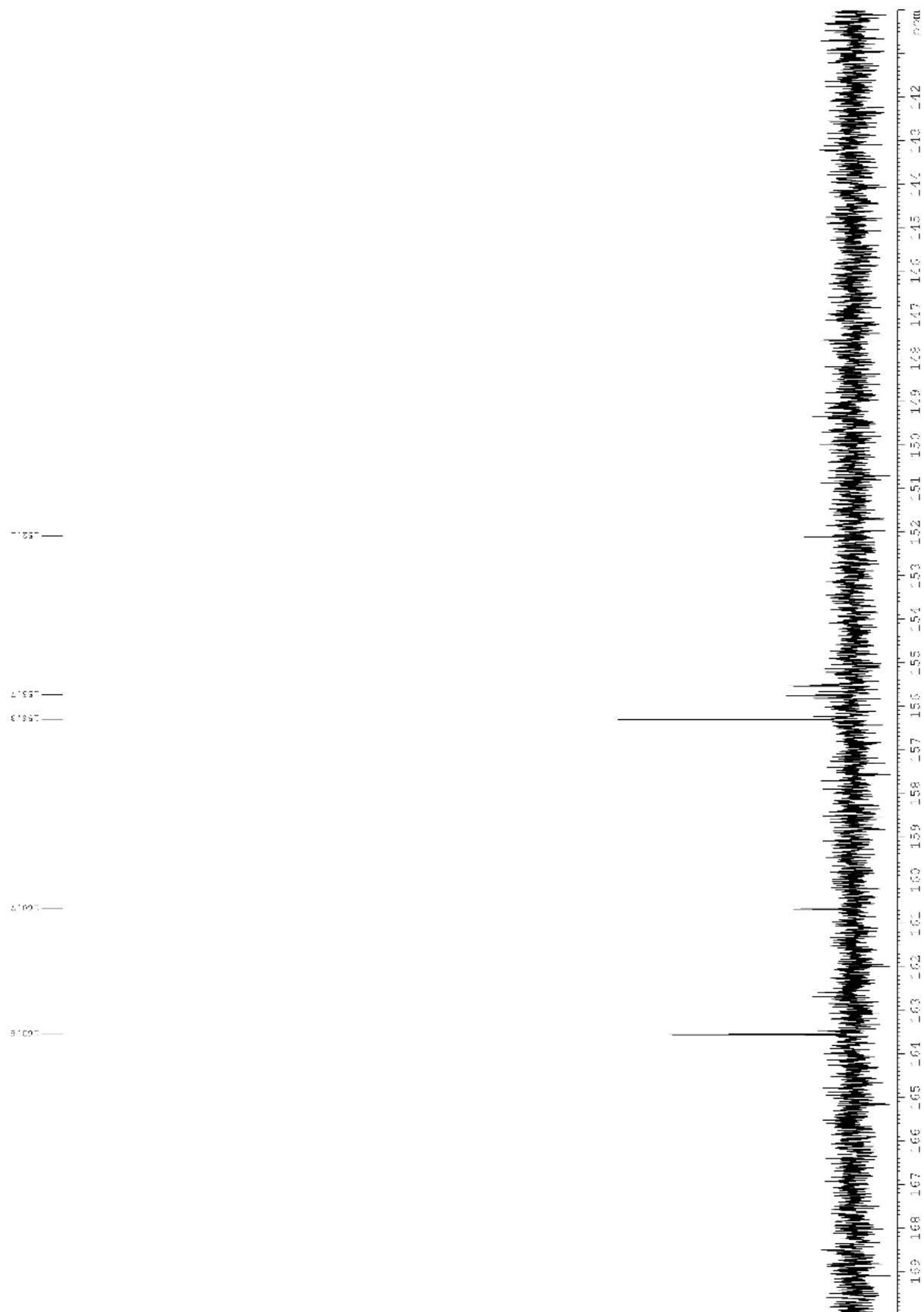**Figure S7c** The ^{13}C NMR spectrum showing the peak at 160.3 ppm

Figure S7d A zoomed in region of the HSQC (with non-uniform sampling) showing the two correlations A and B.

As the LCMS data indicated there were two mono-hydroxylated species with different retention times present in the plant sample, there could be another isomer present. The NMR data point towards this being 2'-hydroxyflavone:

The evidence for this includes:

In the ^{13}C NMR spectrum there is a peak at 152.1 ppm, which is around the expected shift for the quaternary C2' bearing the hydroxyl group (Figure S7e).

In the HSQC experiment with non-uniform sampling, a peak at 132.6 ppm in the ^{13}C NMR correlates with a peak at 7.41 ppm in the ^1H NMR (A, Figure S7f). These shifts match the expected signal for an aromatic CH which is in a meta position relative to the hydroxyl (i.e. the signal for H4')

In the HSQC experiment with non-uniform sampling, a peak at 124.3 ppm in the ^{13}C NMR correlates with a peak at 7.31 ppm in the ^1H NMR (B, Figure S7f). These shifts match the expected signal for an aromatic CH which is in a para position to the hydroxyl group (i.e. for C5').

Figure S7e A zoomed in region of the HSQC (with non-uniform sampling) showing the two correlations A and B.
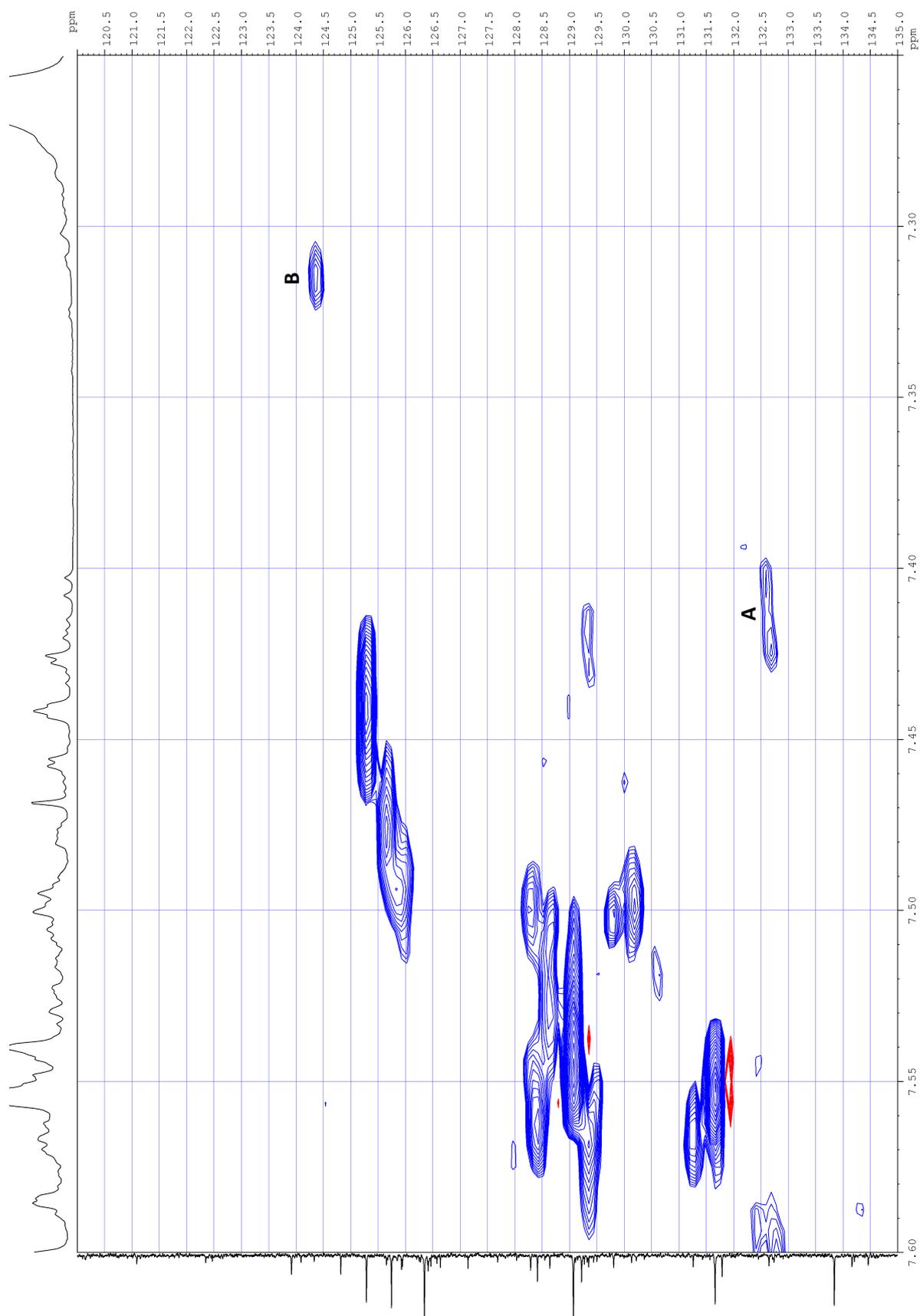
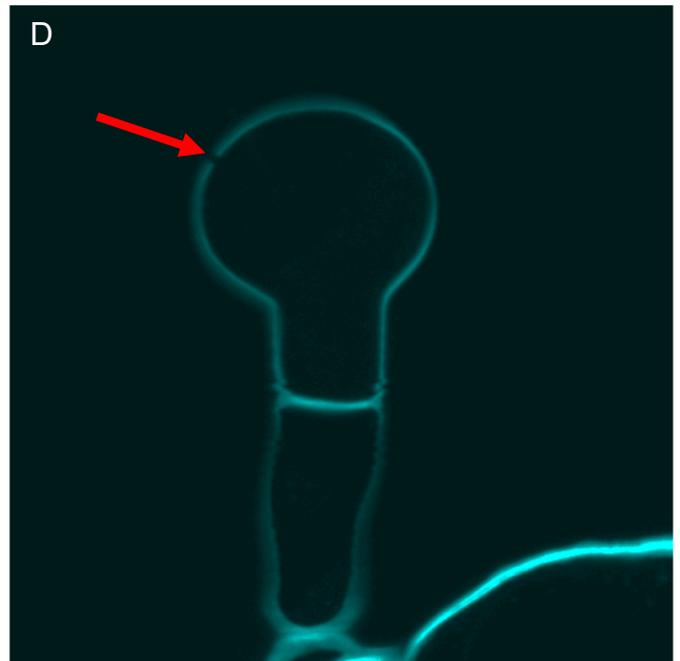**Figure S7f** A zoomed in region of the HSQC (with non-uniform sampling) showing the two correlations A and B.
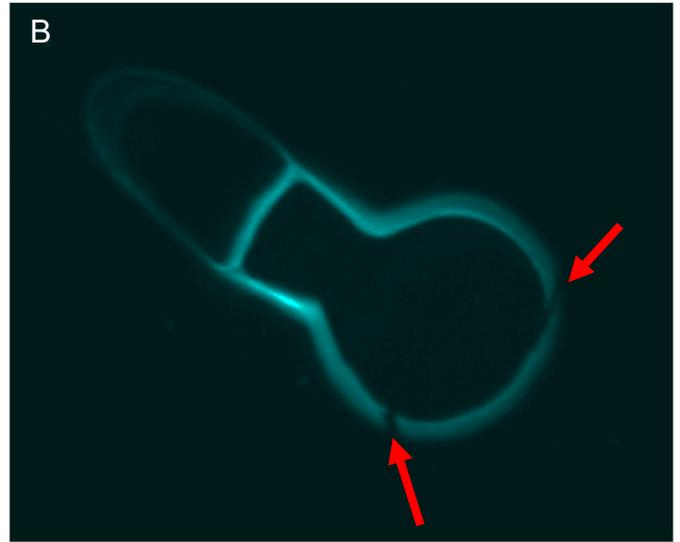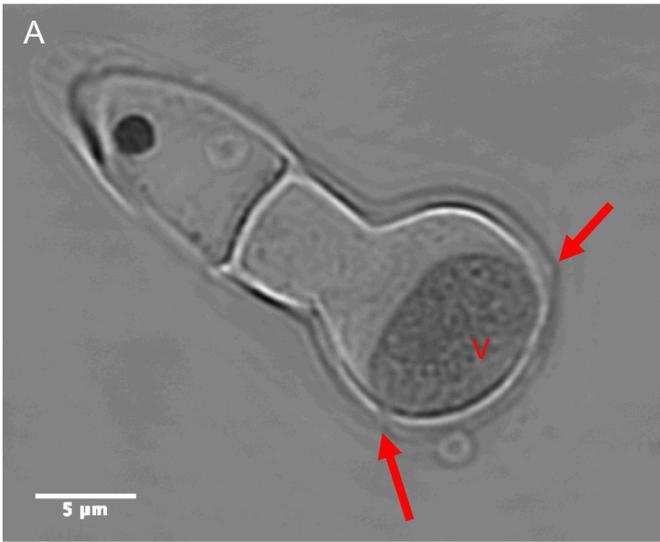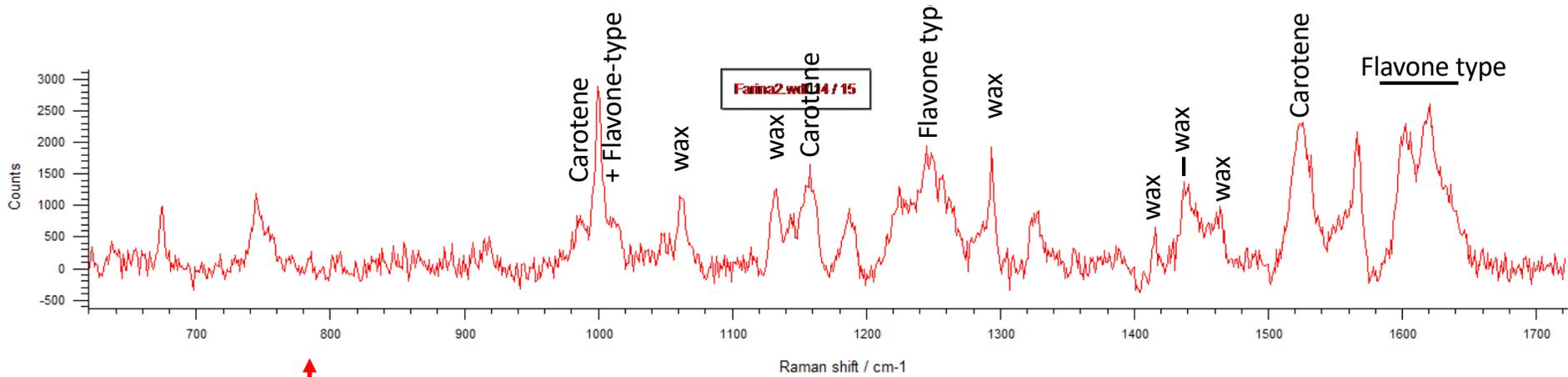
Figure S8. Confocal transmitted image (A, C) and cell wall fluorescence (B, D) of calcofluor-stained sections through gland hair cells. Wool exit holes, observed as discrete gaps in the fluorescence images (arrows) are in close proximity to the dense vacuole (V).
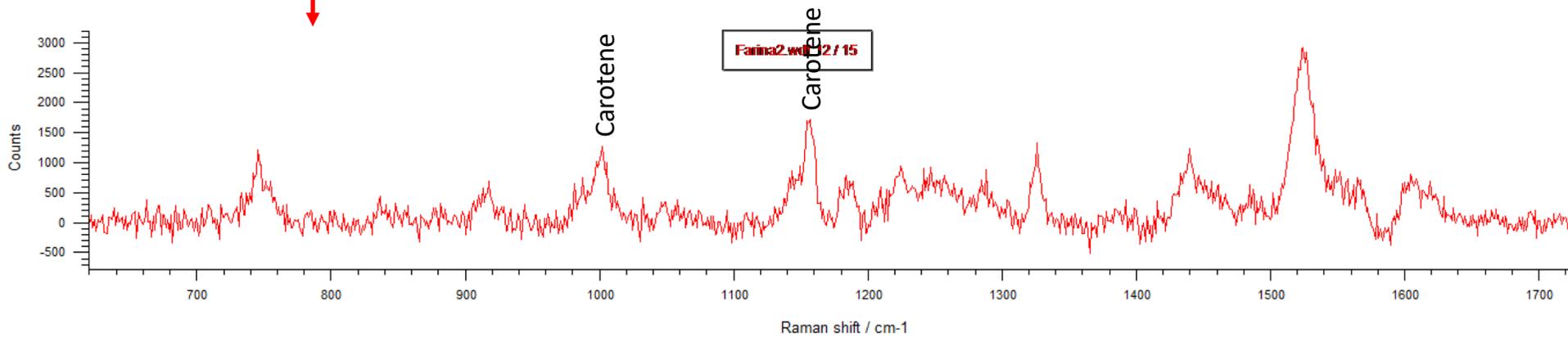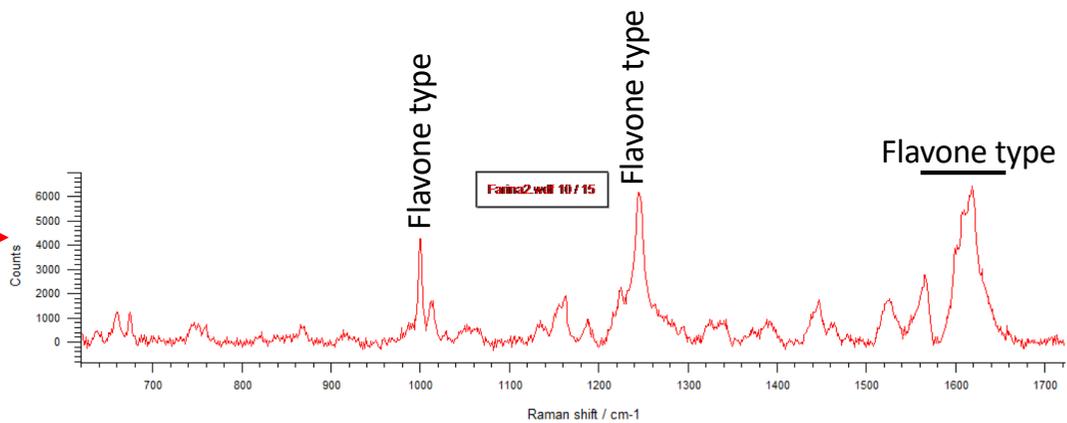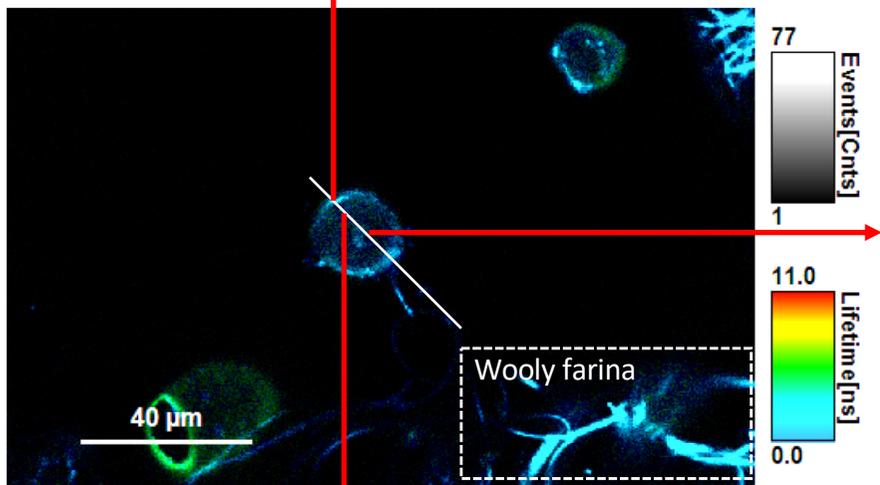
FLIM:

Figure S9. Fluorescence Lifetime Imaging (FLIM) of glandular trichomes taken together with Raman spectra acquired along a line through a trichome cell. The FLIM data (centre left image) represents lifetimes of autofluorescence. Farinose material including the wool and edge of the trichome cell have short lifetimes (cyan and blue colours) with high signal and the cell interior has blue (short) and green (long) lifetimes with low signal. Raman measurements at precise locations along the line confirm the presence of flavone-type material at the cell edge together with strong peaks equivalent to those of plant epicuticular wax (Upper spectrum, assignments are given for prominent peaks). Note the intense cyan labelling in the FLIM image that is a similar lifetime to the wooly farina (white boxed region). Within a proximal location inside the cell there is an absence of the the wax-associated peaks and the strong flavone peaks (lower spectrum). Carotenoid is detected at both locations. Another location inside the cell yielded strong flavone peaks (centre spectrum) and may represent an intracellular store of flavones.